Drought Tolerance Compared Between *Eutrema salsugineum* Genotypes

Drought Tolerance Compared Between Two *Eutrema salsugineum* Ecotypes and Their Recombinant Inbred Lines

By Jennifer R. Tropiano, B.Sc

A Thesis Submitted to the School of Graduate Studies in Partial Fulfillment of the Requirements for the Degree Master of Science

McMaster University
Master of Science (2021)
Hamilton, Ontario (Department of Biology)

TITLE: Drought Tolerance Compared Between Two *Eutrema salsugineum* Ecotypes and Their Recombinant Inbred Lines
AUTHOR: Jennifer R. Tropiano B.Sc (Nipissing University)
SUPERVISOR: Dr. Elizabeth Weretilnyk
NUMBER OF PAGES: xi, 67

Abstract

Despite drought accounting for over 80% of agricultural losses, little progress has been made towards improving drought tolerance in crops. My approach to identifying traits underlying drought tolerance involved a comparison between two accessions of the crucifer, *Eutrema salsugineum*, that display differential tolerance to water deficits. The accessions, originating from the semi-arid Yukon, Canada, and a monsoonal region of Shandong, China, were subjected to a two-step, water deficit and recovery protocol to identify physiological characteristics that discern their drought-responsive behaviour. Traits that discriminate between the ecotypes were used to screen recombinant inbred lines (RILs) that were generated by crossing Yukon and Shandong parent plants. Selected physiological measurements were: anthocyanin accumulation, cut rosette water loss (CRWL), solute potential, relative water content (RWC), static leaf water content (SLWC), specific leaf area (SLA), and OJIP fluorescence emission. Of the measurements taken, CRWL measurements and anthocyanin content distinguished the Yukon ecotype from the Shandong ecotype during the first drought exposure whereas SLA and fluorescence responses differentiated these accessions better after plants that experienced the first drought were rewatered and recovering or undergoing a second drought treatment. Sixty-eight RILs were screened using SLA and OJIP fluorescence emission. SLA and OJIP measurements varied among the recombinant inbred lines (RILs) with many lines showing responses to water deficit intermediate to those of the parental lines. Evidence of heritability in SLA and/or OJIP responses to water deficits would make them useful phenotypic markers for identifying quantitative trait loci (QTLs) associated with drought tolerance in future work.

Table of Contents

LIST OF ABBREVIATIONS

ANOVA analysis of variance

***Chl* a** chlorophyll a

CRWL cut rosette water loss

CW cut weight

D1-10 10% FTSW

D1-40 40% FTSW

D2-10 10% FTSW of a second drought exposure

DW dry weight

ETC electron transport chain

FTSW fraction of transpirable soil water

FW fresh weight

g grams

MPW mean pot weight

ms milliseconds(s)

µL microlitres(s)

mL millitre(s)

MeOH methanol

µs microseconds(s)

PCA principal component analysis

PSI photosystem one

PSII photosystem two

QTL quantitative trait loci

RC reaction center

RILs recombinant inbred lines

ROS reactive oxygen species

RW re-watered

RWC relative water content

SLA specific leaf area

SLWC static leaf water content

SPW saturated pot weight

TW turgid weight

wpg weeks post germination

WPW wilting pot weight

WW well-watered

List of Figures

List of Tables

List of Supplementary Figures

Declaration of Academic Achievement

The research contained in this document has been completed by Jennifer Tropiano with contributions by Dr. Elizabeth Weretilnyk, Dr. Peter Summers, and Anika Chiang. Drs. Elizabeth Weretilnyk and Peter Summers assisted with design and setup of the research project. Dr. Peter Summers collected PSII quantum yield data in 2018 in the Yukon Territory, Canada. Anika Chiang assisted with plant growth and sample collection performed on plants in a second drought exposure. Jennifer Tropiano grew all plants, collected and analyzed data collected from plants at all other stages of drought.

Chapter 1: Literature Review

Drought is a natural condition that results when there is a prolonged period of low precipitation that leads to a shortage of water. Among sources of abiotic stress, drought is considered to be the greatest contributor to reduced yields including crop loss (Boyer, 1982).

1.1 Drought tolerance strategies

Plants can either avoid drought, by not growing in susceptible regions, escape by going to seed, or just tolerate the drought (Yue et al., 2006). Drought avoidance can be seen as a method of postponing the impact of drought when the plant is unable to adequately maintain water levels (Jones and Turner, 1978). Drought tolerant plants must alter their physiological processes in order to withstand this abiotic stress given that reduced water hampers the movement of dissolved solutes, including nutrients, between tissues or cells and even within a cell. Extremophytes are plants that withstand conditions under which most plants fail to thrive including severe drought. Identification of genes conferring drought tolerance using extremophytes and other naturally drought tolerant native plants can be used in molecular breeding for improving drought tolerance of crops (Nuccio et al., 2018).

1.1.1 Anthocyanin accumulation

Anthocyanins are flavonoid pigments that frequently accumulate in plants during reproduction, pollination, as well as during periods of biotic and abiotic stress. Relevant to the subject of this thesis, during water deficits plants frequently increase their content of anthocyanin (Hahlbrock and Scheel, 1989). Stress often leads to the production of reactive oxygen species (ROS), particularly when the capacity of a plant to efficiently use solar energy for photosynthesis is exceeded (Smirnoff, 1993). ROS, in turn, can generate singlet and triplet oxygen species, nitric oxide and other free radicals that can destroy membranes, proteins and other required plant components (Telfer et al., 1994). Anthocyanins have been proposed to serve plants by reducing ROS and/or by providing photoprotective value and signaling functions for plants under stress (Kovinich et al., 2015). However, anthocyanins are a broad class

of related pigments. In *Arabidopsis thaliana* there are about 20 different kinds of anthocyanin pigments found and their accumulation is abiotic condition and tissue-specific (Kovinich et al., 2015). Moreover, Gadjev et al. (2006) used microarray data from multiple ROS-related experiments and monitored the expression of almost 26,000 genes in *Arabidopsis thaliana* exposed to various stress conditions. What they found is the nature of the ROS generator could differentially impact the expression of genes related to anthocyanin synthesis. ROS accumulation attributed to the superoxide anion of oxygen (O_2^{-1}) led to the positive, correlated expression of anthocyanin-related genes, however, this gene expression did not respond to hydrogen peroxide generated in plants deficient in catalase. Thus the role(s) of anthocyanins in protecting plants from stress is likely complex, with regulation and biochemical properties of these pigments still under study.

1.1.2 Response of plants to water deficits

Plants have a variety of methods to regulate their water content allowing them to withstand drought. Stomata close in response to reduced air water vapour content during a drought which saves on transpirational water loss but also decreases carbon dioxide intake and rates of photosynthesis (Flexas and Medrano, 2002). Cavitation, or the formation of emboli in xylem, can increase when plants are stressed which can reduce the volume of water moving from roots to leaves leading to turgor loss (Zhang and Brodribb, 2017; Hsiao et al., 1976). Under drought-induced stress, the active synthesis and accumulation of solutes promotes water uptake to maintain cell turgor (Jones et al., 1980; Morgan, 1980). Under prolonged drought, plants can undergo hydraulic failure when they are no longer able to take up or retain water to maintain turgor (Brodribb and Cochard, 2009; Choat et al., 2012; Cuneo et al., 2016). While plants that tolerate water deficits are able to reduce or prevent water loss, plants have variable capacities to make the adjustments necessary to maintain turgor so plants that survive prolonged drought are usually stunted and far less productive relative to plants given adequate water (Baerenfaller et al., 2012).

1.1.3 Photosynthesis and responses to drought stress

1.1.3.1 General operation of photosynthesis

When light photons are absorbed by chlorophyll, the excitation energy is relayed to either of two reaction centers, photosystem two (PSII) or photosystem one (PSI)

(Figure 1.1) (Zhao et al., 2017). Chlorophylls are associated with these photosystems in an antenna complex where the pigments are bound to chlorophyll binding proteins. Initially, radiant energy captured by the antenna pigments is transferred via resonance transfer to the first site of electron transfer, or photochemistry, at specific chlorophyll a molecules found at reaction centres associated with PSI and PSII. With the excitation of P680 in PSII, a transfer of an electron takes place initiating linear electron flow eventually leading to transfer of an electron to the acceptor associated with PSI (Zhao et al., 2017). The electron "holes" produced at P680 by electron transfer from PSII are filled by electrons released by the splitting of water at PSII. For every pair of electrons leaving PSII, a water molecule is split and for every four electrons generated, a molecule of oxygen is produced along with four protons (H^+) (Zhao et al., 2017). As electrons flow from a high energy system (PSII) to a lower energy system (PSI) they travel through the electron transport chain (ETC) that includes two mobile electron carriers, plastoquinone (QBH_2) and plastocyanin (PC) (Van Eerden et al., 2017). In addition to photochemistry, excited chlorophyll molecules can return to ground state by the emission of energy through the release of heat or light of a higher wavelength (red-shifted) called fluorescence (Zhao et al., 2017). Fluorescence induction and the associated kinetics offers insights into the operation of the photosystems, particularly PSII (reviewed by Stirbet and Govindjee, 2011).

1.1.3.2 The Kautsky effect

When leaves or algae are kept in the dark for a period of time then exposed to light, the fluorescence of chlorophyll a (*Chl* a) takes on a reproducible emission pattern that has been variously called fluorescence induction, fluorescence transient, or the Kautsky effect, named after the German chemist, Hans Kautsky, who began work on this subject in 1931 (Kautsky and Hirsch, 1931; Papageorgiou et al., 1975). Fluorometers are instruments that can be used to measure fluorescence of *Chl* a, many are specifically designed to capture the early and transient aspects of this phenomenon. For evolutionarily advanced plants, *Chl* a fluorescence emission produces a curve comprising a rapidly increasing component followed by a second, slower phase featuring a decreasing slope that is seen within a few minutes (Stirbet and Govindjee, 2011). The fast phase is designated "OJIP" where O stands for origin, the first and minimal level of fluorescence measured, I and J are intermediate levels of fluorescence, and P

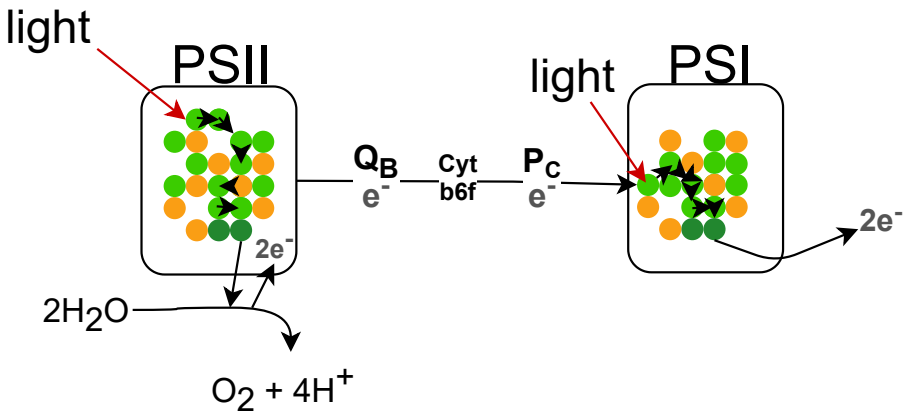

Figure 1.1: Schematic of linear electron flow from PSII to PSI in chloroplast thylakoid membranes. Chlorophyll and carotenoid pigment molecules, symbolized by the green and orange circles, respectively, with the two darker green circles (reaction centers). Electron transfer begins with excitation of P680 at PSII, electrons move from plastoquinone A (Q_A) of PSII by a mobile plastoquinone B (Q_B) to the cytochrome b6f complex (cyt b6f) and then via the mobile carrier plastocyanin (P_C) to P700, the reaction centre chlorophyll a (*Chl* a) of PSI. From PSI electrons are carried via reduced ferredoxin to the terminal electron accepter, $NADP^+$ to produce NADPH.

refers to the final peak fluorescence reached (Stirbet and Govindjee, 2011; Lang et al., 2020).

1.1.3.3 OJIP: A fluorescence response

As described above, a polyphasic fluorescent response called OJIP is generated by dark-adapted samples upon exposure to light (Strasser et al., 2000). After log-transforming time, a typical OJIP graph is produced as shown for a leaf sample from *Eutrema salsugineum* in Figure 1.2. In mechanistic terms, O corresponds to F_O or fluorescence at 2 microseconds(s) (μs) and it describes the minimum fluorescent capacity of PSII. J (F_J) is fluorescence at 2 millisecond(s) (ms), I (F_I) is the fluorescence at 20-30 milliseconds(s) (ms), and P (F_M) is the highest or peak fluorescent value. From the OJIP curve it is possible to elucidate the energy path involving primarily PSII which is enriched in the stacked regions of the thylakoid membranes (the grana)

(Strasser et al., 2000). Fluorescence yield is proposed to reside at the reduction of oxidized Q_A with the availability of this PSII electron acceptor exerting regulatory control over the kinetics of other electron acceptors in the photosynthetic electron transfer chain (Strasser et al., 2000).

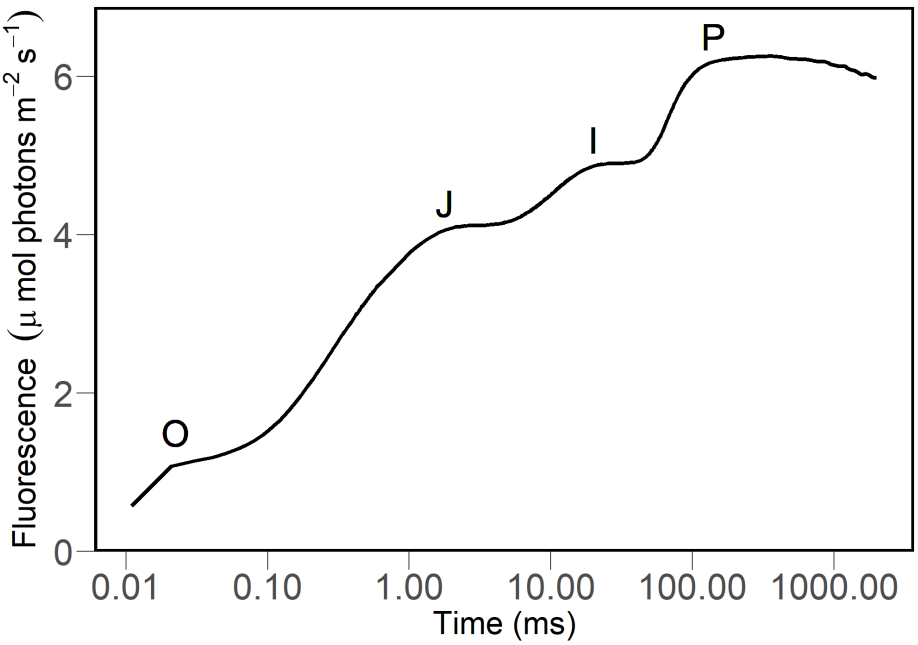

Figure 1.2: The OJIP light response curve produced by leaf tissue of *Eutrema salsugineum* (Yukon ecotype). This graph shows a typical pattern of fluorescence produced as a function of log10 transformed time on the x-axis. The OJIP is a polyphasic curve with an Origin (O), intermediate phases labelled J and I, and a Peak (P).

1.1.3.4 Phasic measurements

Phasic measurements directly derived from the OJIP graph are used to describe the energy flow within chloroplasts (Strasser et al., 2004). The derived values are measurements of fluorescence at specific time points in the OJIP graph: F_O, F_J, F_I, F_M, F_V, Area, and Fixed Area (area between F40μs and F1s). F_O is also known as a plant's dark-adapted ability to take in light when at rest, a point when PSII is fully oxidized or "open" and able to absorb light (Strasser et al., 2004). F_M is the maximal level of light released by fluorescence from chloroplasts, at this point all Q_A is reduced

and all PSIIs are closed. F_V, or variable fluorescence, is determined as the difference between F_M and F_O and this term describes the full dynamic range in fluorescent capability.

Photosystem measurements are used to help explain the impact of a condition on the physiological operations related to photosynthesis and the major source of fluorescence from a leaf at room temperature is PSII (Lichtenthaler et al., 2005; Strasser and Govindjee, 1992). V_J and V_I describe the relative variable fluorescence at J step (or I step) compared to F_V. Frequently used ratios of chlorophyll fluorescence are Fm/Fo, Fv/Fo, and Fv/Fm, with Fv/Fm the most commonly cited value (reviewed by Maxwell and Johnson, 2000). Fv/Fm is the maximum Quantum Yield of photosynthesis and this term describes the efficiency of PSII for photochemistry if all reaction centers (RCs) are open. Comparisons using Fv/Fm are used to assess the efficiency by which PSII operates and decreases in Fv/Fm have been broadly used as an indicator of photoinhibition and in assessing conditions that lead to a decrease in photosynthetic performance (Hughes et al., 2017; Loggini et al., 1999; Zlatev and Yordanov, 2004). For many species, a healthy plant normally has a Fv/Fm value around 0.75 to 0.83 (reviewed by Maxwell and Johnson, 2000 and Guidi et al., 2019) and depression of this value is a reflection of a decrease in the Quantum Yield of PSII due to photoinhibition and indeed any process that dissipates energy such as release of thermal energy (heat) (Guidi et al., 2019).

The ratio Fv/Fo is essentially the same measurement as Fv/Fm and is occasionally used by researchers in addition to Fv/Fm although its more widespread use has been advocated (Lichtenthaler et al., 2005). An advantage of Fv/Fo over Fv/Fm is that the dynamic range covered turns out to be greater and so Fv/Fo is considered to be more sensitive to changes in Quantum Efficiency at the high end, and hence more sensitive to detecting perturbations that decrease Quantum Yield (Lichtenthaler et al., 2005). With negligible use of the Fv/Fo term among scientists, it is difficult to compare results with values reported in the literature whereas Fv/Fm data is readily available for many plants including many stressed plants. The final ratio, Fm/Fo removes the variable component (F_V) and only considers the extremes of the fluorescence emission when RCs are completely open (F_O) or completely closed (F_M) (Strasser et al., 2000). Fm/Fo data are not widely reported in the literature. As time taken to reach maximal fluorescence and time taken to reach relaxation can all be measured, these terms and ratios involving these terms can incorporate a time when

measurements are taken (t) or for transition rates between OJIP stages and/or related flux measurements. These terms can provide additional information about PSII, and indirectly about PSI, which is less prone to photoinhibition relative to PSII yet reliant upon PSII activity for proper functioning (Guidi et al., 2019). Furthermore, devices are available that enable relatively easy lab and field-based measurements that are non-destructive to the plant and so measures of F_O, F_M and F_V are amenable to bulk screening strategies (Kalaji et al., 2014; Kalaji et al., 2017).

1.1.3.5 Measurements of PSII fluctuations

PSII fluorescence fluctuations explain variance in energy related to PSII as this is where electrons begin to flow through the ETC. Accordingly, plants adapt their PSII functioning to suit their environment and measurements can be directed to observe these changes (Strasser and Govindjee, 1992; Strasser et al., 2004). ϕ_{P_O} is the maximal QY of photochemistry derived from F_O and F_M and this term describes the efficiency by which open reaction centers absorb photons, also known as dark-adapted photochemistry (Oukarroum et al., 2009). $\phi_{P_{av}}$ is derived from ϕ_{P_O} (S_M/t_{FM}) where tFM is the time to reach F_M (in ms), and considers ϕ_{P_O} (explained above), and S_M, or the energy needed to close the open RCs. The designation of "M" in S_M refers to multiple turn-overs and considers conditions when more electrons are transferred from Q_{A^-} to the ETC given that S_M increases with a prolonged time that fluorescence is below F_M. This contrasts with S_S, the normalized area for single turnover events. There are measurements that take into account energy fluxes at time = 0, events occurring at the time of chlorophyll excitation. For example, E_O describes the probability that excitation of PSII by a photon will lead to the release of an electron from Q_{A^-} to the ETC (Strasser et al., 2004). The term O measures the efficiency by which an absorbed photon leads to an electron moving past Q_{A^-} and into the ETC whereas ϕ_{D_O} (determined by 1 - P_O – (F_O/F_M)) describes the quantum yield for energy dissipation from thylakoid stacks for both photosystems (Strasser et al., 2000). Thus fluorescence emission provides valuable information about how plants are able to sensitively alter their PSII function in response to a variety of stressors. For example, Oukarroum et al. (2009) applied heat stress to 2-weeks post-germination (wpg) chickpea plants and found the plants typically show a down-regulation of PSII activity and loss of PSII antennae. The measurements above also show how outcomes impacting PSII can be measured using OJIP parameters providing additional information about plant re-

sponses to stress. Importantly, OJIP biphasic curves provide estimates for activities related to PSI and functioning of the ETC as well as PSII (Kalaji et al., 2017; Kalaji et al., 2014).

1.1.3.6 Energy fluctuations

As discussed above, OJIP curves capture features of ETC and fluorescence emission from chlorophyll with deviations offering insights into stress responses of plants. Typically, activities detected by OJIP curves are depressed relative to control values when plants are exposed to environmental stressors (Sunil et al., 2020; Oukarroum et al., 2009). Terms relevant to describing plant responses to environmental conditions include the factor ABS which refers to the photon flux absorbed by chlorophyll pigments associated with the photosystems. The flux ratio $ABS \cdot RC^{-1}$ describes the total number of photons absorbed by chlorophyll pigments associated with all active reaction centres (RC) (Strasser et al., 2000). A change in $ABS \cdot RC^{-1}$ would reflect a change in the number of active relative to inactive RCs with the same photon absorbance. On the other hand, $TR_O \cdot RC^{-1}$ describes the rate whereby an excited electron is trapped by a RC leading to the reduction of Q_A to Q_{A^-} (Hermans et al., 2003; Strasser et al., 2000). $ET_O \cdot RC^{-1}$ represents the transmission of excitation energy to the electron transport chain per RC beyond Q_{A^-}. In addition, $DI_O \cdot RC^{-1}$ is the total dissipated energy of untrapped excitation energy per RC which is the released energy from all active RCs lost as heat, fluorescence and any means other than the ETC. Many of these parameters explain energy fluctuations of the electron transport chain and hence can be used as stress indicators in plants. For example, Sunil et al. (2020) applied sodium nitroprusside, a nitric oxide donor, as a stress signaling chemical on pea plant (*Pisum sativum*) and found decreases in photosynthetic performance parameters but also noted an increase in $DI_O \cdot RC^{-1}$. This was interpreted as an impairment related to the electron transport chain causing dissipation of energy once it enters the photosystems (Sunil et al., 2020). Various Performance Indexes (PIs) have been devised to assess the impact of different conditions on the energy conserved following the absorption of photons by PSII antennae pigments (Stirbet and Govindjee, 2011). π_{Abs} describes the efficiency of energy conservation from photon absorption as it relates to the reduction of Q_B with a higher π_{Abs} indicating more active RCs engaged in highly efficient energy use. Oukarroum et al. (2009) noted differences in photosynthetic PI (total and π_{Abs}) between two varieties of drought-stressed barley,

indications of how differently the same species can respond to drought with respect to the efficient use of light. Many different methods are available as stress indicators based upon or related to electron transport energy fluctuations derived from the OJIP curve.

1.2 Recombinant inbred lines (RILs)

RILs are products of crosses made between two continually inbred parental lines that are then selfed for several generations until a stable generation is reached that is, at least in theory, homozygous for every allele (Pollard, 2012). Each line has a distinct phenotype linked to its inherited traits making comparisons between lines ideal for genetic studies involving quantitative trait loci (QTL) (Miklas et al., 2001).

1.3 *Eutrema salsugineum*

Eutrema salsugineum, or saltwater cress, is an extremophyte member of the Brassica family, a relative to *Arabidopsis thaliana*, and a model plant for studying abiotic stress tolerance (Amtmann, 2009; Kazachkova et al., 2013). *Eutrema* is closely related to other economically important plants in the Brassica family including canola, a crop contributing $26.5 billion annually to the Canadian economy (LMC International, 2016). *Eutrema* tolerates salt to a high extent, however, two ecotypes of focus in this thesis have contrasting abilities to cope with water deficits conditions, likely reflective of biogeographical differences in their native environments and results of local adaptation (MacLeod et al., 2015) (Figure 1.3). The ecotype that is frequently studied originates from Shandong, China, a temperate region featuring periods of monsoonal rains while the second ecotype, less frequently studied, is found in the subarctic, semi-arid Yukon, Canada and is, by comparison, the ecotype more tolerant to drought (Guevara et al., 2012; MacLeod et al., 2015). With the two ecotypes adapted to habitats differing in soil water content and precipitation, comparisons between their drought-responsive behaviours offers an ideal platform for identifying physiological strategies underlying drought susceptibility and tolerance and the genetic basis associated with these traits (Simopoulos et al., 2020). Genes for drought tolerance are urgently needed for breeding crops that will be better suited to withstand drought, a growing global consequence of climate change (FAO et al., 2017).

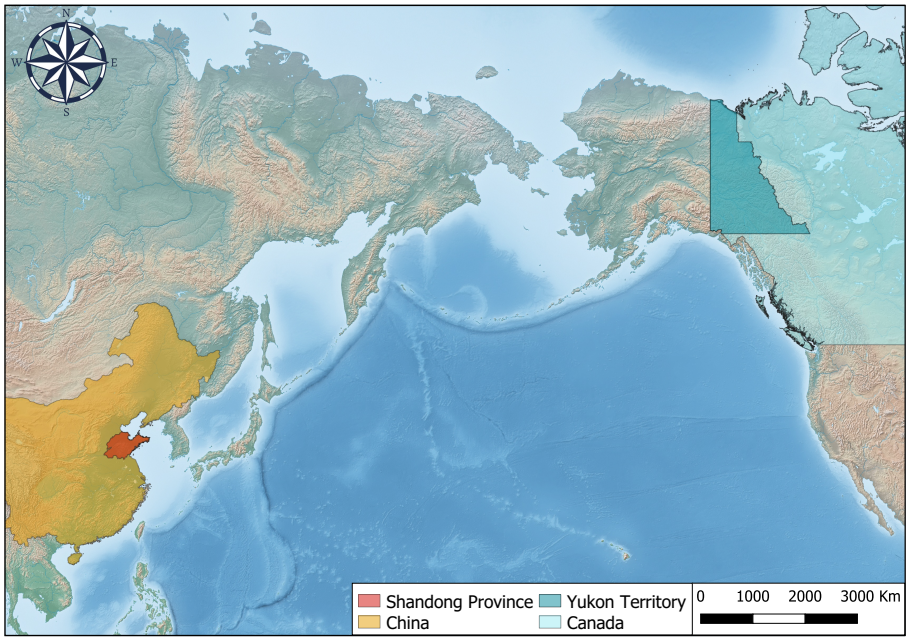

Figure 1.3: Map showing the physical separation of ecotypes from across the Pacific Ocean with Shandong, China to the left and Yukon, Canada to the right. A compass is given at top left and distance scale (km) with legend on the bottom right. Created By: Jennifer R. Tropiano. Geographic Coordinate System: WGS 84 / PDC Mercator. Made with Natural Earth and QGISS (QGIS Team, 2016).

1.4 Research context

A previous study in the Weretilnyk lab by MacLeod et al. (2015) investigated how *Eutrema* responds to successive water deficits. For the drought study, MacLeod et al. (2015) devised a progressive drought treatment protocol whereby water is withheld from plants until plants wilt for an initial drought (D1), the plants are then re-watered (RW) and allowed to recover, and then water is withheld a second time (D2) until a second wilting point is reached. During this protocol, pot weights allow tracking of the water available in the soil for plants to use and this term is the fraction of transpirable soil water (FTSW). As water is withdrawn from soil by the plant or lost by evaporation, pot weight and hence FTSW drops from a high of 100% (well-watered or WW) to 0% when the plants wilt. To evaluate the impact of the progressive drought protocol

on *Eutrema* plants, MacLeod et al. (2015) measured various physiological endpoints including days to wilting, cut rosette water loss (CRWL), anthocyanin content, specific leaf area (SLA), relative water content (RWC), static leaf water content (SLWC), water, pressure, and solute potentials, stomatal conductance, and metabolite profiling using GC-Mass Spectrometry. The physiological comparisons were completed at specific FTSW thresholds during the first or second drought at 40% FTSW (D1-40 and D2-40), a more severe stage at 10% FTSW (D1-10 or D2-10) and during an intermittent re-watering treatment (RW). In comparing Yukon and Shandong plants, the authors determined that Yukon plants were drought tolerant whereas Shandong plants were displaying responses consistent with drought avoidance. In large part, the differences between the ecotypes were not remarkable. Rather, the physiological feature showing the greatest difference between Yukon and Shandong plants was SLA after the second drought exposure. Molecular changes were more sensitive to drought. For example, even at 10% FTSW during the first drought treatment stage (D1-10), and hence before either ecotype had wilted, RT-qPCR showed significant differences in the expression patterns of several classic drought-responsive genes (MacLeod et al., 2015). More recently, RNA-Seq shows those differences in expression patterns include many more genes and that Yukon and Shandong plants undergoing the progressive drought display substantially different transcriptome reprogramming during both drought stages and during re-watering Simopoulos et al. (2020).

1.5 Thesis Hypothesis

Drought tolerance is known to be a complex genetic trait governed by many genes hindering advances in crop improvement (reviewed by Nuccio et al., 2018). For this thesis, my hypothesis is that RILs produced by crossing Yukon and Shandong parent lines will show patterns of drought-responsive behaviour that resemble their Shandong or Yukon parental plants or drought tolerance intermediate to the parental lines. Segregating RILs showing the high drought-coping ability of the Yukon parental line should share genetic signatures responsible for this trait with the Yukon genotype. However, what will be important to testing this hypothesis will be access to a convenient, scalable procedure to reliably assess differences in drought tolerance among the many RILs available for screening.

1.6 Thesis Objectives

My approach uses the physiological variability among RILs and their Yukon and Shandong parental plants with respect to drought tolerance. All measurements compared well-watered control plants against drought-treated plants of the same maturity to ensure that responses are not confounded by differences in development. MacLeod et al. (2015) identified several traits that distinguish parental plants that experienced drought from those that did not, but the traits were not necessarily suitable for screening many lines. Many of the measurements done by MacLeod et al. (2015) used destructive sampling and also were not amenable for testing many plants of each line to maximize the chance of detecting minor but statistically significant differences in stress-responsive behaviour. Moreover, the physiological traits that discriminated Yukon from Shandong plants were best observed following a second drought exposure which adds to the complexity of the screen in terms of labour (not all plants wilt simultaneously) and space needed for testing. However, RNA-Seq analysis of plants undergoing the progressive water deficit protocol show that both ecotypes undergo transcriptome remodeling during the first stage of the two-step protocol and that the extent to which this happens is very different between the ecotypes (Simopoulos et al., 2020). Phenotypic markers that can be applied to differentiate the ecotypes and RILs during the first drought stage would be useful both in shortening the length of the experiment and in perhaps identifying different QTLs associated with first versus subsequent water deficit exposures.

The objectives of this study included:

- A review and expansion of the physiological screening tools developed by MacLeod et al. (2015) and evaluation of their suitability in distinguishing between Yukon and Shandong plants. For this work, much of the emphasis is placed on the first stage of the progressive drought protocol and the re-watering stage.
    - Initial tests to include measurements used by MacLeod et al. (2015): cut rosette water loss (CRWL), anthocyanin content, solute potential, relative water content (RWC), static leaf water content (SLWC), and specific leaf area (SLA).
    - Testing to expand the screening tools available to evaluate the suitability of measuring OJIP fluorescence and related terms (eg. Fv/Fm).

- To apply screens found to be most effective towards evaluating the drought tolerance variability among RILs.

Chapter 2: Materials and Methods

2.1 Plant growth conditions

2.1.1 Seed Source and Reagents

Yukon and Shandong *Eutrema salsugineum* ((Pall.) Al-Shehbaz & Warwick) parental lines and RILs were selected from the Weretilnyk lab seed catalogue. All lines originated in the lab of Dr. Barbara Moffatt (U. Waterloo, ON, Canada) and have been maintained and bulked periodically at McMaster University. Years previously, several single-seed decent lines were generated from a single parental line and five of those lines representing each ecotype were chosen at random for use in this study. The catalogue numbers for these lines, preceded by Y and S for the Yukon and Shandong ecotypes respectively, are: Y1, Y4, Y6, and Y8, Y11 and S2, S3, S7, S15, and S16.

Unless otherwise specified, all chemicals used were supplied by MilliporeSigma (Oakville, ON) and the plant growth products (including fertilizer) were purchased from Plant Products Inc. (Ancaster, ON). Where reference is made to H_2O, this is exclusively water purified using a Centra R200 Water Purification System and this source was used in the preparation of solutions and for watering plants.

2.1.2 Seed Sterilization

Approximately 50 seeds were sterilized in a microfuge tube by first suspending seeds with 1 mL 70% (v/v) ethanol for 2 min. The ethanol was removed and seeds were rinsed with H_2O before adding 1 mL of 0.1% (v/v) Triton X-100 in 5% bleach diluted to 50% strength. After 2 min the seeds were rinsed with H_2O four times until no more bubbles were visible. Sterilized seeds were suspended in 0.1% (w/v) sterile Phytagel overnight for approximately 12 hours at 4°C.

2.1.3 Plant Growth Conditions

Seeds suspended in Phytagel (see 2.1.2) were transferred to 6x6x9 cm pots filled with 170 to 180 grams (g), moistened, lightly packed soil mixture. The soil mixture was prepared according to Velasco et al. (2016) and contained 71% (v/v) sphagnum peat moss (Premier Tech, Rivièredu-Loup, PQ, Canada), 14% (v/v) Turface® MVP Soil Conditioner (Profile, Buffalo Grove, IL, USA), 10% (v/v) coarse grade perlite (Pre-

mier, New Eagle, PA, USA), 5% (v/v) medium vermiculite (Therm-O-Rock), 1.85% (w/v) dolomite lime (Natural Lime & Stone), and 25% (v/v) H_2O. The moistened soil was autoclaved at 121°C for 30 min, once the mixture cooled 1.5 L of AquaGro 2000G was added (1.85 mL AquaGro 2000G in 1.5 L H_2O; Aquatrols, Paulsboro, NJ, USA) as a wetting agent and to help retain a high capacity for the soil to re-wet after drought treatment. Approximately 3 to 5 seeds were sown onto the soil surface of each pot and lightly covered with soil mixture. Pots were placed into arrays of 32 within trays, the trays were covered with plastic lids to ensure high humidity during germination and then the trays were moved into a 4°C cold room for either 4 d (Yukon) or 7 d (Shandong and RILs) to synchronize germination. After the cold treatment under dark conditions, trays were moved to a growth chamber set to 21°C, 21 h days at 250 $\mu mol^{-2}s^{-2}$ light intensity and 10°C, 3 h nights. The plastic lids were removed after 7 d and plants were watered as needed and fertilized once per week with a 1 g per L solution of 20-20-20 (N-P-K) fertilizer. When seedlings developed 2 to 4 leaves, seedlings were thinned to one plant per pot, typically this was done at 7 d post-germination (dpg).

2.2 Drought Treatment Protocol

A replicate was comprised of a minimum of 40 plants per ecotype. Treatments were randomly assigned to 20 plants of each ecotype. Four plants from each of the five single-seed decent parental lines underwent a water deficit exposure. Twenty additional plants, four plants from each of the five single-seed decent parental lines, served as consistently well-watered negative controls. The two-stage drought protocol followed was as reported by MacLeod et al. (2015). The progressive drought protocol was started by withholding water from the plants at 4 weeks post germination (wpg)(Figure 2.4). Control plants that were continually watered did not receive fertilizer while plants undergoing drought were left unwatered. Soil water loss was monitored to track the experiment progression using FTSW (fraction of transpirable soil water) (MacLeod et al., 2015; Sinclair & Ludlow, 1986). FTSW was converted to a percentage (0 to 100%) as described by Equation 2.1. FTSW considers soil water at saturation (saturated pot weight or SPW), mean pot weight (MPW) during a period where water is withheld, and pot weight when plants wilt determined as the wilting pot weight (WPW). Where two successive drought treatments were used, plants were watered and given a 48-hour recovery period before the second drought exposure. Re-

watering before the second drought was performed by replenishing water needed to restore half the FTSW associated with saturation on the first day with the remainder given on the second day. While re-watering the second day the plants were fertilized with 1 g per L of 20-20-20 (N-P-K) fertilizer and well-watered controls were fertilized as well.

$$FTSW = \left(\frac{MPW - WPW}{SPW - WPW}\right) * 100 \qquad \text{Equation 2.1}$$

2.3 Sampling

Destructive sampling was performed between 14:00 and 16:00, times corresponding to 8 and 10 hr into the day cycle. Destructive sampling procedures included severing roots from shoots for the CRWL assay or tissue removal for storage at -80°C for future assays (RNA analysis or anthocyanin determination). Tissue collection was done using a razor blade and tweezers with approximately 150 mg of leaf tissue removed from each plant and transferred to a sterile, labeled microfuge tube (identified by plant line, sample number, and date). The tubes with tissue were immersed in liquid N_2 to flash-freeze the contents for storage at -80°C. Plants used for destructive sampling were not used for subsequent measurements. For the non-destructive measurements, including OJIP determinations, plants were temporarily removed from the growth cabinets, placed on a table in the same room for measurements and then the plant was returned to the cabinet as quickly as possible until the plant was used for other determinations. For example, plants used for OJIP sampling at the various stages were also used for SLA measurements prior to harvest.

2.4 Details of Measurements

2.4.1 OJIP determinations

A FluorPen FP 100 portable fluorometer (Photon Systems Instruments, PSI, Czech Republic) was used to determine OJIP values following the manufacture's instructions. Measurements were performed outside of the growth cabinets. Leaf clips were attached to the most recently fully-expanded leaf of a plant. The cuvette cover was closed to dark-adapt the leaf for 15 min (Figure 2.1). Next, the fluorometer unit was placed on the clip and measurements for the OJIP curve were obtained. A second

measurement was then taken from the second most recently fully-expanded leaf on the same plant. FluorPen software version 1.1.1.1 was used to calculate 24 values in addition to fluorescence at four OJIP phasic points (Table 3.1; Strasser et al., 2000). The two measurements from the leaves of each plant were averaged for a representative value of the plant.

Figure 2.1: Detachable leaf clips on expanded leaves of a Yukon *Eutrema* plant for OJIP measurements. During dark adaptation a metal tab in the window of the clip is set in a closed position and for measurements the tab slides away to expose the leaf to light.

2.4.2 Anthocyanin Content

Anthocyanin was extracted from leaves frozen in liquid nitrogen using the method of Kim et al. (2003) as cited by Velasco et al. (2016) for *Eutrema*. A fully-expanded leaf was put into a 2 mL microcentrifuge tube. The leaf was submersed in 1 mL

extraction solution (1% HCl in methanol (MeOH)) for 24 hours at 4°C. Next, 200 microlitres(s) (μL) H_2O and 200 μL chloroform were added and the contents of the tube were mixed by inverting the microcentrifuge tube a few times. The tubes were centrifuged at 15, 800g for 1 min for phase separation. The aqueous supernatant was transferred to a glass cuvette and the absorbance measured at 530 and 657 nm using a Thermo Scientific™GENESYS™20 Visible Spectrophotometer. Anthocyanin content was determined using Equation 2.2 from Kim et al. (2003).

$$Anthocyanin = \frac{A530 - 0.33 \times A657}{FW} \qquad \text{Equation 2.2}$$

2.4.3 Cut Rosette Water Loss (CRWL) Assay

CRWL was assayed by cutting the rosette at the base using a scalpel, near the root-shoot junction, then measuring the fresh weight (FW) of the severed shoot on a Mettler analytical balance. Severed shoots were suspended in air over a weigh boat and after 180 min, biomass was determined again providing the cut weight (CW) (Figure 2.2) (MacLeod et al., 2015). CRWL was calculated using Equation 2.3.

$$CRWL = 100\left(\frac{100}{FW}\right) \times CW \qquad \text{Equation 2.3}$$

Figure 2.2: Processing CRWL samples at D1-40 for the Yukon accession. Each rosette in respective weigh boats after FW has been collected. Labels placed in front of each boat with sample indentifiers.

2.4.4 Solute Potential Determinations

Solute potential (ψ_s) was determined as described by Weretilnyk et al. (1995) and MacLeod et al. (2015). Measurements were made using a Wescor psychrometer fitted with C52 chambers. A standard curve was generated to calibrate the sample chambers using filter paper discs and solutions of 0.15, 0.3, 0.4, 0.5, 0.6, 0.7, and 0.8 M NaCl. Leaf discs (6 mm diameter) were excised from a recently fully-expanded leaf using a cork borer, the discs were then flash-frozen in liquid N_2. Leaf discs were allowed to thaw and then the thawed leaf disc was placed in the chamber and allowed to equilibrate for 20 min. Dew point measurements were recorded and the standard curve generated earlier was used to derive ψ_s estimates.

2.4.5 Specific Leaf Area Measurements

In this study SLA was measured using the fresh weight of a whole rosette, in contrast to using rosette dry weight for this determination (MacLeod et al., 2015). A photo of the entire rosette was taken using a Canon EOS Rebel T3 digital single-lens reflex camera (DSLR). The rosette image was analyzed for area using a python script to automate ImageJ analysis (https://github.com/JennTropiano/MScThesis) (Abràmoff et al., 2004). The whole rosette was severed from the roots at the base and fresh mass was determined as described previously for the CRWL assay. SLA was calculated using Equation 2.4.

$$SLA = \frac{Area(m^2)}{Rosette\ Mass(g)} \times 100 \qquad \text{Equation 2.4}$$

2.4.6 Relative and Static Leaf Water Content (RWC and SLWC)

RWC and SLWC measurements were collected simultaneously. A recently, fully-expanded leaf was used to obtain discs (6 mm diameter) using a #3 cork borer. The FW biomass was obtained using an analytical balance and three replicate discs were pooled and put into a 1.5 millitre(s) (mL) microcentrifuge tube with 1 mL H_2O. After 18 hr at ambient laboratory conditions, turgid weight (TW) was obtained. Microcentrifuge tubes with the leaf discs were then put in an oven for 72 hr at 65°C

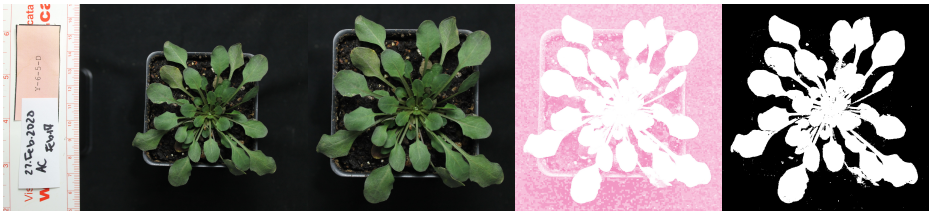

Figure 2.3: Step-wise process for Specific Leaf Area (SLA) determinations using Image J. Image analysis process shown from left (raw image) to right (processed format): 1. raw image with a ruler to scale pixel density, 2. previous image now cropped to show the plant in its pot, 3. previous image adjusted to turn green hues white and non-green colours pink, and 4. image threshold switched to black and white where the pink is now black and the white area is easily quantified.

and a final dry weight (DW) was measured. Two calculations were made from these measurements: RWC (Equation 2.5) and SLWC (Equation 2.6):

$$RWC = \frac{FW - DW}{TW - DW} \times 100 \qquad \text{Equation 2.5}$$

$$SLWC = \frac{FW - DW}{DW} \qquad \text{Equation 2.6}$$

2.4.7 Statistical Analysis

All data collected had two factor treatments, by genotype (Shandong, Yukon, or RILs) and by treatment (drought-exposed or well-watered). Analysis of data was done using R version 3.6.0 (RStudio Team, 2020). Principal Component Analysis (PCA) and analysis of variance (ANOVA) were performed with the base R stats package (R version 3.6.0; RStudio Team (2020)). Significance was indicated by $p < 0.05$ (*) with any p values lower than 0.01 denoted by multiple asterisks: ** < 0.01, *** < 0.001, **** < 0.001. Post-hoc tests were conducted using Tukey's HSD (honestly significant difference) from the base R stats package (R Core Team, 2019).

2.5 Drought Treatment Protocol

Figure 2.4 shows a schematic summary of the progressive drought treatment protocol used for this thesis and identifies the periods when measurements and/or samples

were taken. Plants at D1-10 and D2-10 represent plants that are in soil with very low available water in that the FTSW is only 10% the level present in the soil of a consistently well-watered plant. Moreover, plants at D2-10 have already undergone one period of wilting (FTSW at 0%) and recovery after being re-watered (RW). Despite the severity of the stress, Figure 2.4a shows that both Yukon and Shandong plants grew during this progressive drought with both ecotypes having more leaves by the D2-10 stage compared to the onset of the treatment at 4 wpg, a feature also reported by MacLeod et al. (2015) using the same protocol.

Not all determinations used in this study were completed at the various stages shown in Figure 2.4. For example, CRWL and anthocyanin content determinations were taken at D1-40 (40% FTSW), solute potential at D1-10 (10% FTSW), SLA, RWC, and SLWC were all measured at RW, and SLA at D2-10 (10% FTSW). These measurements made it possible to test the reproducibility of the drought stress procedure devised and published by MacLeod et al. (2015) and its impact on *Eutrema* using plant lines and growth cabinets that we currently have. However, we expanded the tests to include OJIP fluorescence measurements which can be easily performed at any of the progressive drought treatment stages without losing plants to destructive sampling and allowed us to re-sample plants at several stages of the progressive drought protocol without injuring the plants. The information provided by OJIP fluorescence are provided by variables listed in Table 3.1. Many of these measurements were discussed in Chapter 1 but a short description of each variable is also included in Table 3.1.

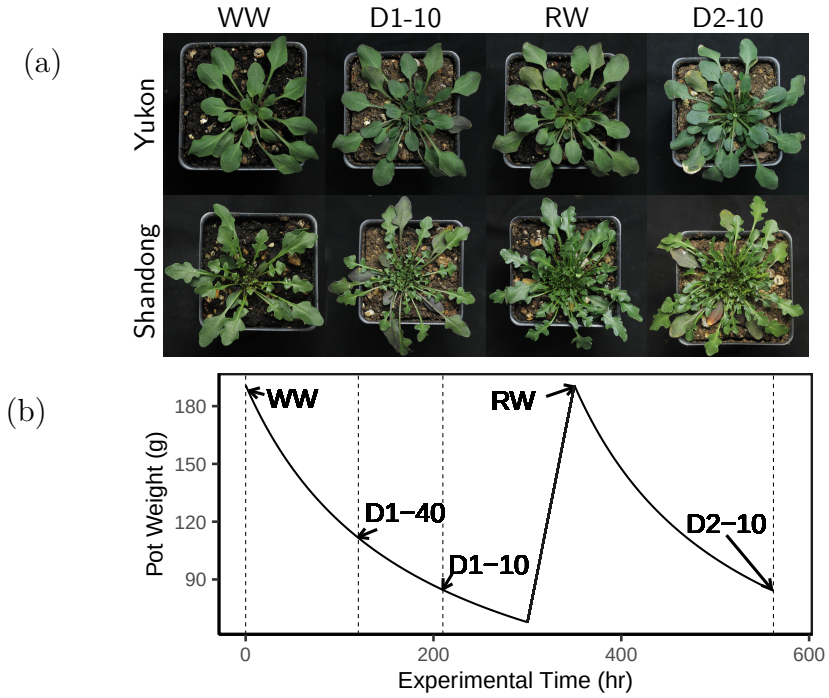

Figure 2.4: Progressive drought treatment for testing water deficit tolerance of *E. salsugineum* plants. (a) Representative Yukon and Shandong plants shown at various stages of the progressive drought treatment protocol (see Materials and Methods for details) with designated stages corresponding to FTSW values. (b) Designations for the sampling time points used for various measurements described in this thesis: WW (100% FTSW), D1-40 (40% FTSW), D1-10 (10% FTSW), RW (re-watered), D2-10 (10% FTSW) of the second drought exposure. Approximate times for the stages that plants reach time points are shown on the x axis.

Chapter 3: Results

Shandong and Yukon Eutrema plants underwent two successive water deficits separated by a 48 hour recovery period to evaluate parameters to screen RILs. CRWL and anthocyanin content were taken at 40% FTSW (D1-40), solute potential at 10% FTSW (D1-10), SLA, RWC, and SLWC at RW, and SLA at 10% FTSW of a second drought exposure (D2-10). OJIP fluorescence was also taken at all stages. Variables measured from OJIP fluorescence are listed in Table 3.1.

Table 3.1: OJIP variables listed on the left with a brief description of their contribution to the polyphasic fluorescence response.

Variable	Description
F_O	Fluorescence intensity at 50μs, minimum dark-adapted fluorescence
F_J	Fluorescence intensity at J-step (2 ms)
F_I	Fluorescence intensity at I-step (60 ms)
F_M	Maximal fluorescence
F_V	Maximal variable fluorescence
Area	Area between fluorescence curve and F_M with background subtracted
Fixed Area	Area below the fluorescence curve between F40μs and F1s(background subtracted)
HACH Area	For manufacturer's use
V_I	Relative variable fluorescence at J-step
V_J	Relative variable fluorescence at I-step
F_M/F_O	Ratio of maximal to minimal fluorescence
F_V/F_O	Active fluorescence ratio
M_O	Approximate value of the initial slope for the relative variable fluorescence curve
S_M	Multiple turn-over
S_S	Single turn-over as the smallest possible S_M
N	Turn-over number of Q_A
PSII Quantum Yield	Maximal efficiency of PSII (Φ), calculated as $F_V \cdot F_M^{-1}$
ϕ_{P_o}	Maximal yield of dark-adapted photochemistry
ψ_{P_o}	Probability of a trapped electron moving to the ETC after Q_A
ϕ_{E_o}	Rate constant for intersystem electron transport kE
ϕ_{D_o}	Energy dissipation quantum yield
$\phi_{P_{av}}$	Time to reach maximal fluorescence
π_{Abs}	Absorption performance index of PSII
$ABS \cdot RC^{-1}$	Absorbance of the reaction center
$TR_O \cdot RC^{-1}$	Trapped energy energy fluctuation per RC
$ET_O \cdot RC^{-1}$	Electron transport energy fluctuation per RC
$DI_O \cdot RC^{-1}$	Dissipated energy energy fluctuation per RC

3.1 D1-40: Mild drought exposure

Cut rosette water loss (CRWL) at D1-40 in Shandong plants was 1.8-fold higher relative to well-watered (WW) Shandong plants whereas there was no significant difference between WW and D1-40 Yukon plants (Figure 3.1(a)). Comparing the Shandong drought exposed plants, which had no difference in anthocyanin relative to WW plants, Yukon plants had on average 5.3-fold more anthocyanin at D1-40 than WW Yukon plants and 9.5-fold more anthocyanin than WW or D1-40 Shandong plants (Figure 3.1(b)).

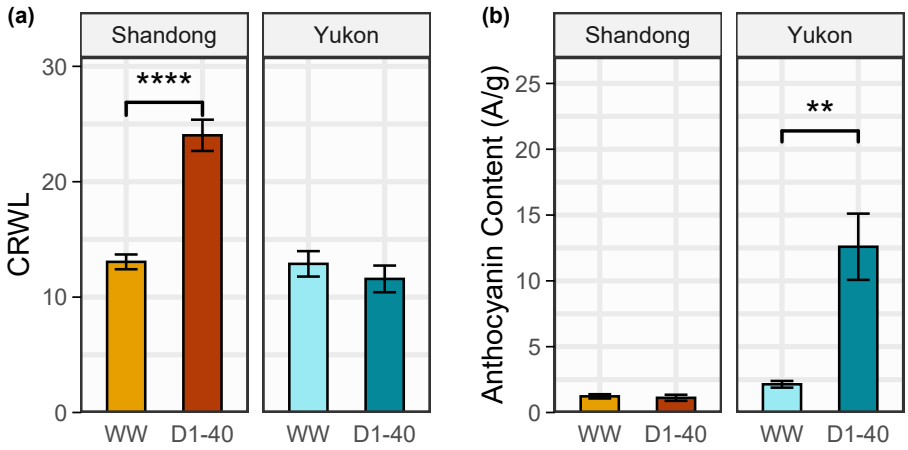

Figure 3.1: Shandong and Yukon plants show contrasting water loss and anthocyanin accumulation at D1-40 stage of progressive drought protocol. Mean ± SEM with five biological replicates for 10 WW and D1-40 plants, n=20 plants for each ecotype.

Principal component analysis (PCA) was used to visualize OJIP data collected for plants of both ecotypes at each of each of four stages of the progressive drought protocol (Figure 3.2). In these analyses, PC1 and PC2 together explained, on average, about 80% of the variation in the data. Figure 3.2(a) visualizes data for both ecotypes that have been exposed to a D1-40 stage of drought treatment. PC1 largely separates the scores corresponding to ecotype. However, while the scores for Shandong WW and D1-40 plants overlap, the same is not true for Yukon plants where scores of D1-40 plants are positioned more positive to the origin along the PC2 axis relative to those of Yukon WW plants. The Figure 3.2(a) biplot shows that scores for OJIP data can

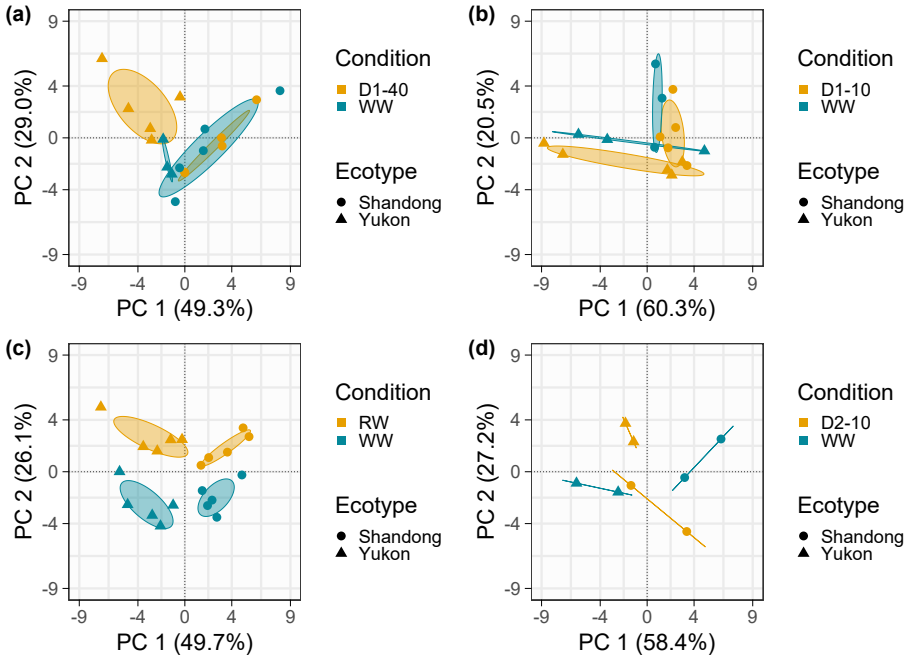

Figure 3.2: PCA biplots comparing ecotype responses to drought using OJIP data from well-watered (WW) and drought-treated (D) plants at four stages: (a) D1-40, (b) D1-10, (c) RW, and (d) D2-10. Ellipses represent 50% confidence euclidean distribution. Five replicates per ecotype for (a), (b), and (c) (n=20) and two replicates representing each ecotype for (d) (n=4).

better distinguish Yukon WW from D-40 plants than the corresponding data collected from Shandong plants.

The PCA biplot shown in Figure 3.2(b) describes OJIP data produced using plants experiencing the more severe, D1-10 water deficit stage. Some overlap along PC2 is seen between the distributions of scores for Yukon WW and D1-10 plants, however, data for the latter occupies more negative positions along PC2 relative to the data generated from WW Yukon plants. The distribution of scores for Shandong WW and D1-10 OJIP data shows greater overlap suggesting that the main sources of variance captured by PC1 and PC2 for OJIP measurements are not useful signatures for discerning Shandong control and drought-treated plants.

Figure 3.2(c) visualizes the OJIP data for WW and RW plants and, in this case, the biplot produced leads to clusters that are separated along PC1 on the basis of ecotype and along PC2 with respect to treatment. Both ecotypes show the same treatment-specific clustering distribution relative to the origin making RW treatment and OJIP data a promising combination to discriminate genotypes on the basis of their recovery from D1 during RW. The PC factor loadings for the biplot shown in Figure 3.2(c) are listed in Table 3.2. For PC1, Fv/Fm, ϕ_{P_O}, Fm/Fo and Fv/F share the highest positive values while ϕ_{D_O} has the most negative value. Thus the factors associated with ratios of chlorophyll fluorescence have the greatest positive impact and the quantum yield for energy dissipation (ϕ_{D_O}) the greatest negative factor loading that discerns the ecotypes along PC1. Along PC2, the greatest positive factor loading that separates treatment data is attributed to F_J (the fluorescence level at 2ms or J-level see 1.1.3.3) and the most negative observation being S_S (normalized area for single turnover events, see 1.1.3.5).

The biplot of Figure 3.2(a) groups scores for genotype and provides the best drought related separation of scores, albeit only for Yukon plants. The PC factor loadings for Figure 3.2(a) are shown in Table 3.3. For PC1, the fluorescence ratios (Fv/Fm, Fm/Fo, and Fv/Fo) and ϕ_{P_O} share the highest positive loading values and ϕ_{D_O} has the most negative factor loading value. Along PC2, which shows the greatest separation related to drought for Yukon plants, the greatest positive loading factor is S_S (normalized area for single turnover events, see 1.1.3.5) and the greatest negative loading factor is F_I (the fluorescence level at 60 ms, or I-step, see 1.1.3.3).

The factor loadings describing the greatest variability along PC2 of Figure 3.2(c) suggests that Yukon plants recovering from drought (RW) can be discriminated from

Table 3.2: First six Principal Component factor loadings corresponding to biplot of Figure 3.2(c) showing OJIP data for WW and RW Shandong and Yukon plants.

	PC1	PC2	PC3	PC4	PC5	PC6
$F_V \cdot F_M^{-1}$	0.244	0.015	-0.001	-0.008	0.017	-0.002
ϕ_{P_o}	0.244	0.015	-0.001	-0.008	0.017	-0.002
$F_M \cdot F_O^{-1}$	0.244	-0.001	0.007	-0.055	-0.021	-0.021
$F_V \cdot F_O^{-1}$	0.244	-0.001	0.007	-0.055	-0.021	-0.021
ϕ_{E_o}	0.235	-0.047	-0.045	0.199	-0.010	-0.066
π_{Abs}	0.232	-0.103	-0.048	-0.008	-0.128	-0.125
ψ_o	0.231	-0.052	-0.054	0.244	-0.007	-0.071
$ET_O \cdot RC^{-1}$	0.218	0.044	-0.034	0.369	0.031	-0.046
HACH Area	0.206	0.220	0.079	-0.089	-0.026	-0.035
F_V	0.205	0.224	0.065	-0.093	-0.016	-0.031
Fixed Area	0.181	0.275	0.090	-0.109	-0.037	-0.045
F_M	0.181	0.277	0.076	-0.114	-0.027	-0.041
F_I	0.147	0.307	0.074	-0.106	-0.199	-0.292
Area	0.110	0.204	-0.440	-0.164	0.112	-0.070
S_S	0.076	-0.339	-0.068	-0.407	-0.141	-0.089
S_M	-0.037	0.048	-0.588	-0.103	0.163	-0.062
N	-0.055	0.156	-0.543	0.019	0.183	-0.031
$TR_O \cdot RC^{-1}$	-0.061	0.353	0.055	0.411	0.084	0.038
F_J	-0.076	0.356	0.109	-0.350	-0.018	0.026
F_O	-0.154	0.318	0.064	-0.119	-0.066	-0.061
V_I	-0.170	-0.075	-0.029	0.071	-0.418	-0.683
$ABS \cdot RC^{-1}$	-0.182	0.242	0.039	0.291	0.035	0.017
$\phi_{P_{av}}$	-0.201	0.036	-0.104	0.129	-0.071	-0.387
M_O	-0.227	0.143	0.059	-0.118	0.016	0.061
V_J	-0.231	0.052	0.054	-0.244	0.007	0.071
$DI_O \cdot RC^{-1}$	-0.240	0.063	0.011	0.087	-0.022	-0.008
ϕ_{D_o}	-0.244	-0.015	0.001	0.008	-0.017	0.002

Table 3.3: First five Principal Component factor loadings corresponding to biplot of Figure 3.2(a) showing OJIP data for WW and D1-40 Shandong and Yukon plants.

	PC1	PC2	PC3	PC4	PC5
ϕ_{D_o}	-0.247	-0.029	0.048	-0.046	-0.004
M_O	-0.241	-0.062	-0.084	-0.064	-0.146
$DI_O \cdot RC^{-1}$	-0.232	-0.137	0.106	-0.060	-0.004
V_J	-0.209	0.147	-0.234	-0.023	-0.153
V_I	-0.204	0.078	-0.131	-0.035	0.710
F_O	-0.195	-0.254	-0.118	-0.138	-0.044
$ABS \cdot RC^{-1}$	-0.181	-0.277	0.183	-0.085	-0.031
$TR_O \cdot RC^{-1}$	-0.128	-0.350	0.220	-0.094	-0.047
$\phi_{P_{av}}$	-0.120	0.130	-0.003	-0.460	0.295
F_J	-0.110	-0.100	-0.450	-0.114	-0.209
F_I	0.041	-0.287	-0.368	-0.145	0.422
N	0.084	0.115	0.200	-0.552	-0.101
$ET_O \cdot RC^{-1}$	0.126	-0.295	0.317	-0.029	0.108
S_M	0.126	0.254	0.076	-0.442	-0.071
S_S	0.129	0.346	-0.221	0.101	0.098
Fixed Area	0.166	-0.281	-0.228	-0.110	-0.063
F_M	0.169	-0.276	-0.225	-0.109	-0.087
Area	0.192	0.121	-0.014	-0.391	-0.100
HACH Area	0.207	-0.201	-0.186	-0.069	-0.049
F_V	0.209	-0.197	-0.183	-0.068	-0.071
ψ_o	0.209	-0.147	0.234	0.023	0.153
ϕ_{E_o}	0.222	-0.124	0.193	0.023	0.134
π_{Abs}	0.237	-0.030	0.079	0.032	0.173
$F_M \cdot F_O^{-1}$	0.246	0.039	-0.053	0.049	0.012
$F_V \cdot F_O^{-1}$	0.246	0.039	-0.053	0.049	0.012
$F_V \cdot F_M^{-1}$	0.247	0.029	-0.048	0.046	0.004
ϕ_{P_o}	0.247	0.029	-0.048	0.046	0.004

WW control plants on the basis of altered photosynthetic properties for which S_S and F_I were the greatest sources of variability. S_S describes the number of times Q_A is reduced and reoxidized between F_O and F_M whereas F_I is fluorescence at 2ms (Stirbet and Govindjee, 2011).

Finally, Figure 3.2(d) shows preliminary results for a D2-10 treatment. There were fewer replicates because the experiment was stopped early for the COVID-19 lockdown. However, while this experiment should be repeated, the data already suggests that OJIP data in the biplot clusters scores for Yukon WW from D2-10 plants along PC2 while the same is not the case for the corresponding scores of Shandong WW and D2-10 plants.

Figure 3.3 shows a PCA biplot generated from data collected for the D1-40 stage of the progressive drought protocol. In contrast to Figure 3.2(a), the analysis used to generate the Figure 3.3 biplot included CRWL and anthocyanin content data in addition to OJIP measurements. This analysis was done to determine if additional phenotypic data would improve the clustering shown in Figure 3.2(a). Figure 3.3 shows that PC1 and PC2 together account for 85% of the variance in the data, which reflects a greater contribution from PC1 (about 61%) relative to PC1 in Figure 3.2(a) (approximately 49%). There is, moreover, a tighter clustering of scores that separate ecotype along PC1 with all of the Shandong scores lying positive and Yukon scores negative relative to the origin along the x axis, respectively. On the other hand, PC2 shows a separation of the scores for both ecotypes by treatment with all D1-40 scores above the y axis origin and WW scores below. A review of the factor loadings associated with the data of Figure 3.3 is shown in Table 3.4. M_O, approximate value of the initial slope for the relative variable fluorescence curve, and π_{Abs}, absorptive performance index of PSII, were the observations with the highest positive and negative factor loadings, respectively, for PC1. S_S and $ET_O \cdot RC^{-1}$ (electron transport energy fluctuation per reaction center) were the highest positive and negative factor loadings for PC2, respectively. Table 3.4 also shows that anthocyanin has the highest positive contribution to factor loadings of PC3 whereas CRWL contributes most highly to PC2. In summary, including anthocyanin content and the CRWL assay with OJIP data led to an improved clustering of scores by ecotype and treatment relative to the biplot that used only OJIP data shown in Figure 3.2(a). This suggests that including CRWL and anthocyanin content with OJIP fluorescence can better discern Shandong and Yukon WW from D1-40 plants.

Table 3.4: First five Principal Component factor loadings for Shandong and Yukon *Eutrema* plants at D1-40 using CRWL, anthocyanin, and OJIP data corresponding to biplot of Figure 3.3.

	PC1	PC2	PC3	PC4	PC5
M_O	-0.2319	0.0768	-0.0328	-0.0127	-0.0103
ϕ_{D_o}	-0.2283	0.0981	-0.0053	-0.0694	-0.0244
V_I	-0.2075	-0.1674	-0.0642	0.0803	0.0637
F_O	-0.2011	0.1925	-0.0803	0.0082	-0.0482
$DI_O \cdot RC^{-1}$	-0.1996	0.1967	0.0696	-0.0849	0.0002
F_J	-0.1981	-0.0536	-0.2890	0.2006	-0.0969
V_J	-0.1941	-0.1947	-0.1461	0.0681	-0.0472
Anthocyanin	-0.1910	0.1085	0.2779	-0.0732	-0.0668
$\phi_{P_{av}}$	-0.1592	-0.0214	-0.4103	-0.2457	-0.0302
$ABS \cdot RC^{-1}$	-0.1479	0.2872	0.0862	-0.0892	0.0269
F_I	-0.1452	0.1390	-0.3201	0.3893	0.0042
$TR_O \cdot RC^{-1}$	-0.1117	0.3248	0.0912	-0.0874	0.0406
$ET_O \cdot RC^{-1}$	0.0836	0.3371	0.1484	-0.0981	0.0614
Fixed Area	0.1100	0.2860	-0.1997	0.2707	-0.0598
S_S	0.1108	-0.3279	-0.0666	0.0905	-0.0407
F_M	0.1172	0.2851	-0.1916	0.2447	-0.0646
N	0.1210	0.1531	-0.3147	-0.4736	0.0501
CRWL	0.1526	0.2368	-0.1558	-0.0158	-0.0830
S_M	0.1717	-0.0763	-0.3132	-0.3546	0.0427
ψ_o	0.1941	0.1947	0.1461	-0.0681	0.0472
Area	0.1969	-0.0118	-0.2919	-0.2500	0.0087
HACH Area	0.1982	0.1579	-0.1373	0.2365	-0.0291
F_V	0.2005	0.1595	-0.1308	0.2125	-0.0339
ϕ_{E_o}	0.2091	0.1573	0.1333	-0.0466	0.0430
$F_V \cdot F_O^{-1}$	0.2280	-0.0914	0.0595	0.0741	0.0155
$F_M \cdot F_O^{-1}$	0.2280	-0.0914	0.0595	0.0741	0.0155
$F_V \cdot F_M^{-1}$	0.2283	-0.0981	0.0053	0.0694	0.0244
ϕ_{P_o}	0.2283	-0.0981	0.0053	0.0694	0.0244
π_{Abs}	0.2300	0.0376	0.1299	-0.0013	0.0104

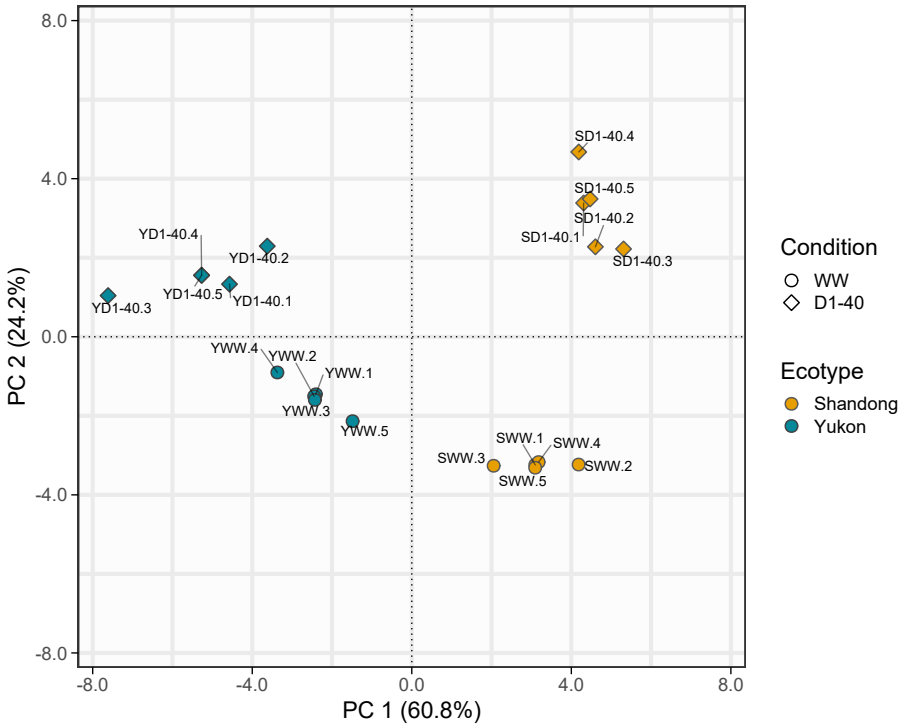

Figure 3.3: PC1 and PC2 biplot for combined CRWL, anthocyanin, and OJIP fluorescence measurements of control (WW) and D1-40 *Eutrema* plants. (5 replicates, n=20)

3.2 D1-10: First severe drought exposure

During the more severe D1-10 stage of the drought treatment, Yukon plants underwent a statistically significant decrease in solute potential relative to WW plants while no comparable change was found for Shandong plants (Figure 3.4). The reader should note that the data plotted in Figure 3.4 is shown as -MPa.

A PCA was conducted using OJIP data and solute potential measurements. This was done to determine whether including solute potential, a physiological measurement, could improve the data visualised in Figure 3.2(b) for WW and D1-10 plants. The PCA biplot displayed in Figure 3.5 shows that PC1 and PC2 describe, collectively, about 79% of the variance in the data, which compares well relative to 80% for PC1 and PC2 in Figure 3.2(b). However, whereas Figure 3.2(b) showed a separation between scores of Yukon WW and D1-40 plants, Figure 3.5 now better separates scores of Shandong plants along PC2 while the scores of Yukon plants are less well

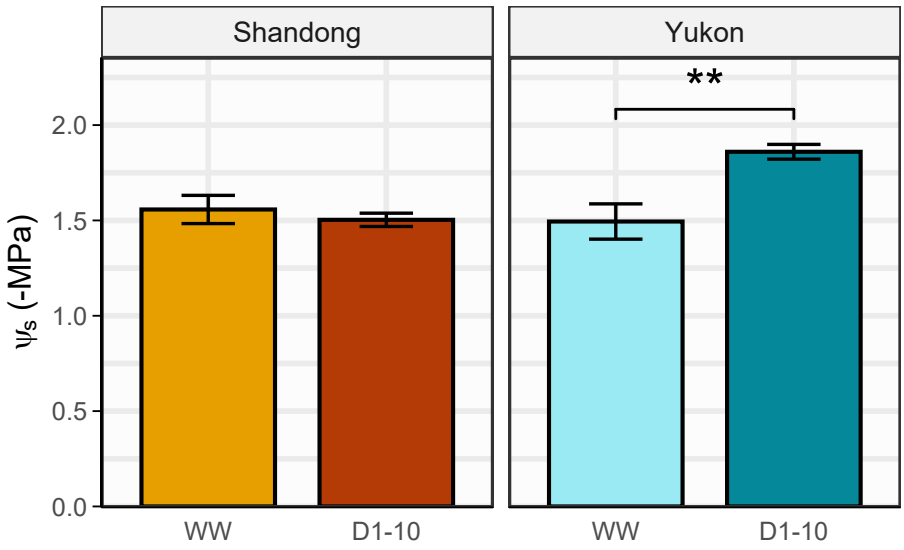

Figure 3.4: Solute potential measurements for leaves of Shandong and Yukon *Eutrema* plants at the D1-10 stage of the progressive drought treatment. Bars are ± SEM of five biological replicates for WW and D1-10 plants (n=20).

grouped by treatment relative to the PCA biplot in Figure 3.2(b) that only used OJIP data.

Looking at the factor loadings from data shown Figure 3.5, ϕ_{D_O} (energy dissipation quantum yield) was the observation with the most negative factor loading and ϕ_{P_O} (maximal yield of dark-adapted photochemistry) as well as Fv/Fm (PSII quantum yield or the maximal efficiency of PSII) was the most positive value for PC1. N, turnover number of Q_A, and S_S were the most positive and negative factor loadings for PC2, respectively. In Table 3.5 solute potential contributed 0.1039 to PC1. In summary, by including solute potential to the OJIP data, clustering of scores by ecotype and treatment improved compared to using only OJIP data alone as in Figure 3.2(b), but only by clustering data related to Shandong plants by treatment.

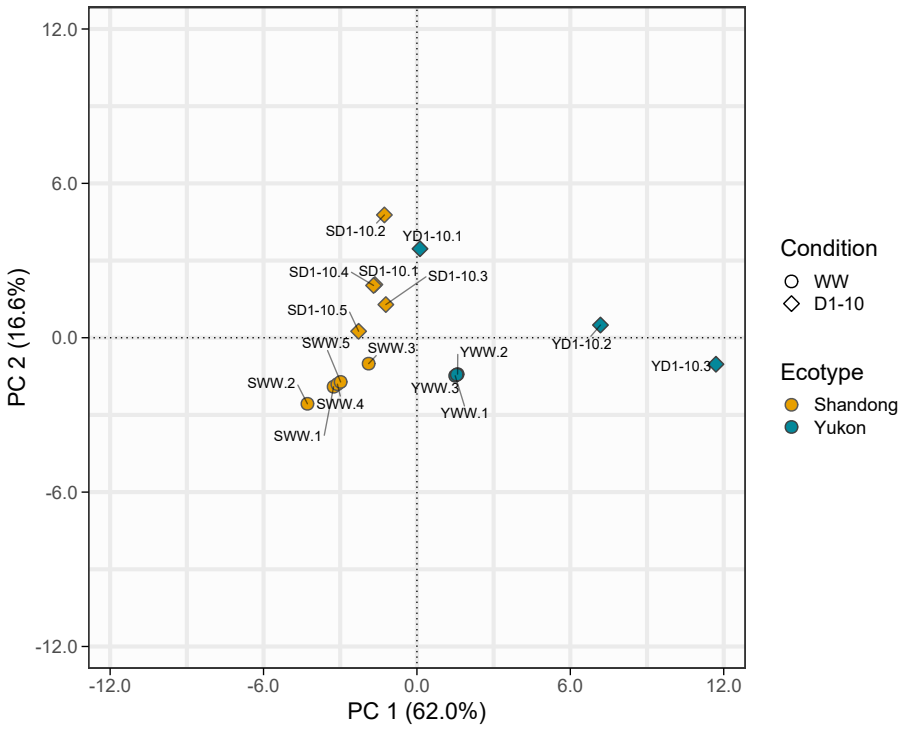

Figure 3.5: PCA biplot of solute potential and OJIP data comparing drought exposed Yukon and Shandong plants at WW and D1-10 (5 replicates, n=10)

Table 3.5: First five Principal Component factor loadings at D1-10 including solute potential and OJIP data of parental plants.

	PC1	PC2	PC3	PC4	PC5
ϕ_{D_o}	-0.2375	0.0557	-0.0183	0.0091	-0.0394
M_O	-0.2370	-0.0415	-0.0332	0.0582	-0.0333
$DI_O \cdot RC^{-1}$	-0.2266	0.1312	-0.0662	-0.0361	-0.0841
V_I	-0.2244	-0.0763	0.0457	0.0976	0.0563
F_O	-0.2239	0.0483	-0.1703	0.0704	-0.0382
$\phi_{P_{av}}$	-0.2031	0.2030	0.0244	0.1836	0.1550
V_J	-0.2016	-0.2278	0.0757	0.1186	0.0249
$ABS \cdot RC^{-1}$	-0.1857	0.2480	-0.1622	-0.0714	-0.0915
F_J	-0.1736	-0.2630	-0.1235	0.2224	0.0341
$TR_O \cdot RC^{-1}$	-0.1396	0.3145	-0.2205	-0.0911	-0.0893
F_I	-0.0502	-0.1256	-0.4367	0.2728	0.0217
N	0.0052	0.3975	0.1350	0.3038	0.1437
S_M	0.0772	0.2736	0.2601	0.3691	0.2111
Solute Potential	0.1039	-0.0679	0.0035	0.4696	-0.1131
$ET_O \cdot RC^{-1}$	0.1224	0.3504	-0.1778	-0.1527	-0.0513
S_S	0.1406	-0.3147	0.2232	0.0652	0.0657
Fixed Area	0.1437	-0.0336	-0.3978	0.1742	-0.0386
Area	0.1491	0.2209	0.1476	0.3751	0.1811
F_M	0.1500	-0.0391	-0.3862	0.1734	-0.0389
ψ_o	0.2016	0.2278	-0.0757	-0.1186	-0.0249
HACH Area	0.2094	-0.0472	-0.2370	0.1056	-0.0136
F_V	0.2103	-0.0506	-0.2321	0.1067	-0.0147
ϕ_{E_o}	0.2133	0.1918	-0.0598	-0.1085	-0.0262
π_{Abs}	0.2310	0.0772	0.0531	-0.1072	-0.1002
$F_V \cdot F_O^{-1}$	0.2342	-0.0752	0.0565	-0.0301	-0.0262
$F_M \cdot F_O^{-1}$	0.2342	-0.0752	0.0565	-0.0301	-0.0262
$F_V \cdot F_M^{-1}$	0.2375	-0.0557	0.0183	-0.0091	0.0394
ϕ_{P_o}	0.2375	-0.0557	0.0183	-0.0091	0.0394

3.3 Recovery after a first drought exposure

Relative water content (RWC) and static leaf water content (SLWC) were measured on plants after experiencing a water deficit and two days of recovery to determine stress responsive behavioural differences between the ecotypes. The typical ranges for both ecotypes RWC measurements ranged between 67% and 84% and for SLWC the range was between 4 and 6 (Figure 3.6). In Figure 3.6 there was no significant difference found between water deficit recovered plants and WW control plants for either RW or SLWC measurements. There was also found to be no significant difference of well-watered control plants of either ecotype for RWC and SLWC.

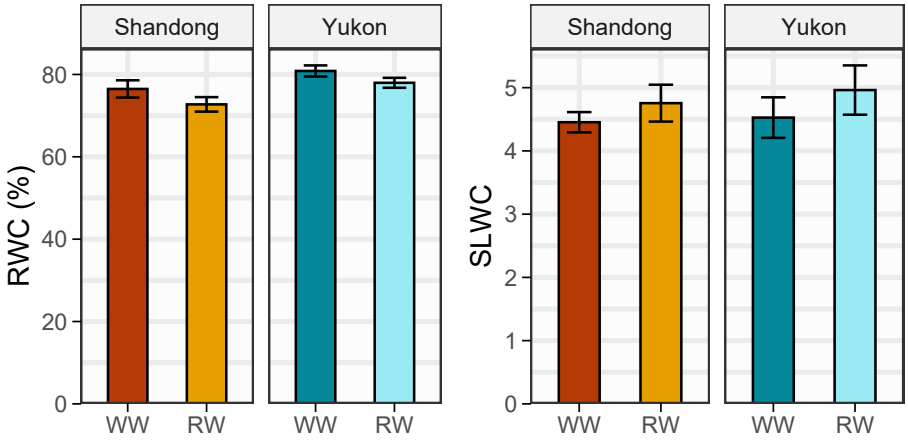

Figure 3.6: Relative water content (RWC) and static leaf water content (SLWC) measurements of *Eutrema* parental lines at RW. Bars represent ± SEM of five biological replicates for Shandong and Yukon well-watered and drought-exposed plants (n=20).

The PCA biplot shown in Figure 3.2(c) displayed a separation of the OJIP data based upon ecotypes and treatment with PC1 and PC2 accounting for about 76% of the variation. When SLA, RWC, and SLWC measurements were included in a PCA, PC1 and PC2 accounted for about 75% (Figure 3.7). A notable change for the PCA of Figure 3.7 relative to the one shown in Figure 3.2(c) is a reduction in the variation accounting for PC2 from 26 to 19% respectively, and a reduced separation between the scores of WW and RW Shandong plants. Thus inclusion of SLA, RWC, SLWC values did little to improve the clustering that was produced using only OJIP data (Figure 3.7 and Figure 3.2(c)).

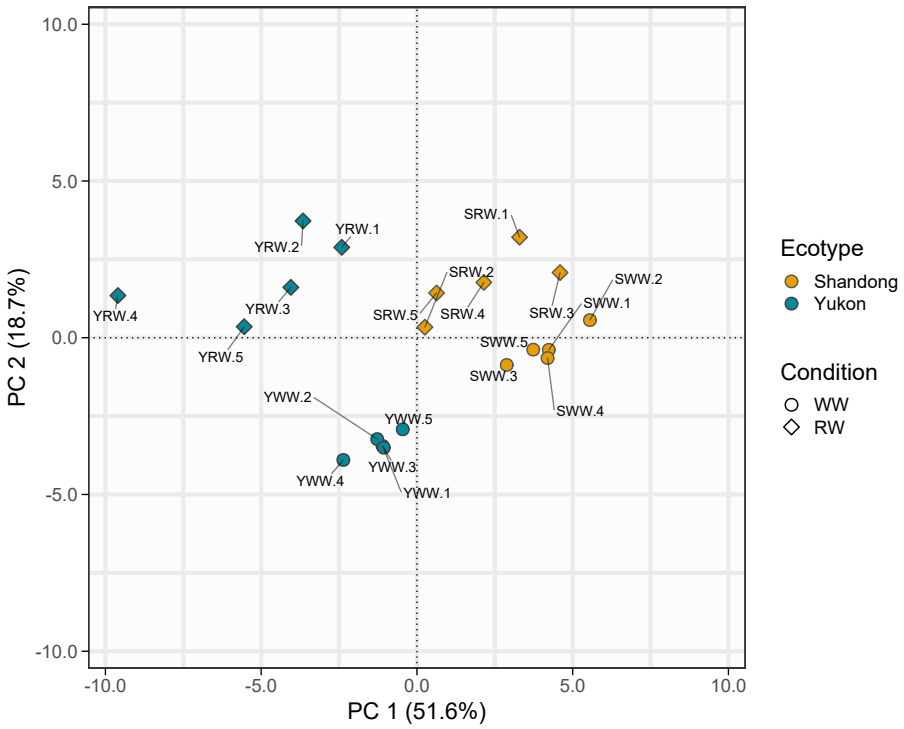

Figure 3.7: PCA biplot of SLA, RWC, SLWC, and OJIP fluorescence data for WW and RW Yukon and Shandong plants (5 replicates, n=20)

3.4 Differential responses to a second severe drought

At D2-10, specific leaf area (SLA) was measured to compare leaf expansion between Shandong and Yukon plants after a recovery to a water deficit (Figure 3.8). Yukon RW plants had a higher SLA (17.3 $cm^2 \cdot g^{-1}$) relative to WW plants (12.6 $cm^2 \cdot g^{-1}$). Of note, there was no significant difference in SLA measurements between WW and RW Shandong plants. SLA values for Yukon plants at the D2-10 treatment stage were also higher relative to WW plants at 16.1 $cm^2 \cdot g^{-1}$ and 13.8 $cm^2 \cdot g^{-1}$, respectively, whereas Shandong plants were not significantly different with respect to SLA at 11.5 $cm^2 \cdot g^{-1}$ for D2-10 plants and 12.2 $cm^2 \cdot g^{-1}$ for WW plants.

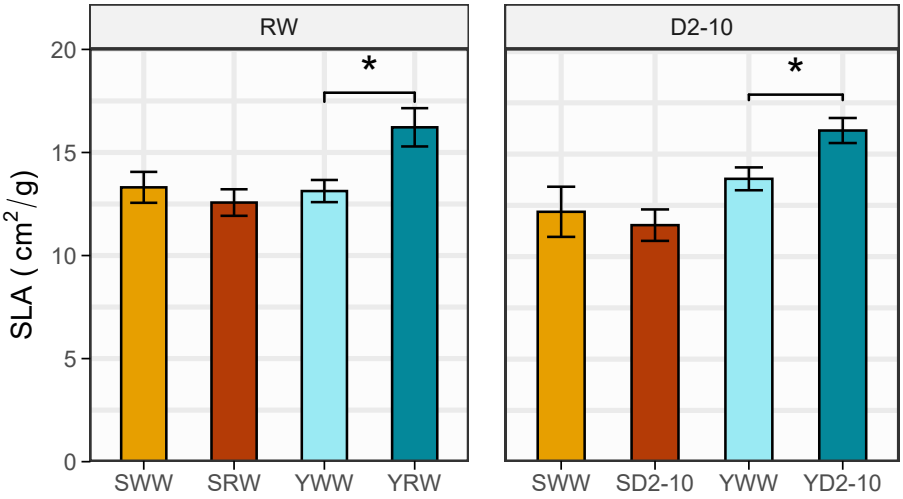

Figure 3.8: Specific leaf area (SLA) for plants at RW and D2-10 stages of the progressive water deficit treatment relative to WW controls. SLA measurements for *E. salsugineum* ecotypes at RW and D2-10 stages of treatment reported with SLA values for age-matched control WW plants. Bars are ± SEM of 5 biological replicates for RW and 2 for D2-10 (n=20).

The PCA biplot produced for data representing the D2-10 data relative to data for WW plant (Figure 3.2(d)) was amended to include SLA data (summarised in Figure 3.8) and is shown in Figure 3.9. PC1 and PC2 again account for about 86% of the variance when SLA data is included but the Yukon WW and D2-10 data show an improved separation along the PC2 axis with data for plants clustered positively to the origin and scores for D2-10 plants below the origin while the opposite pattern

is shown for Shandong plants (Figure 3.9). This use of SLA data at D2-10 could help resolve RILs from Yukon or Shandong parent phenotypes.

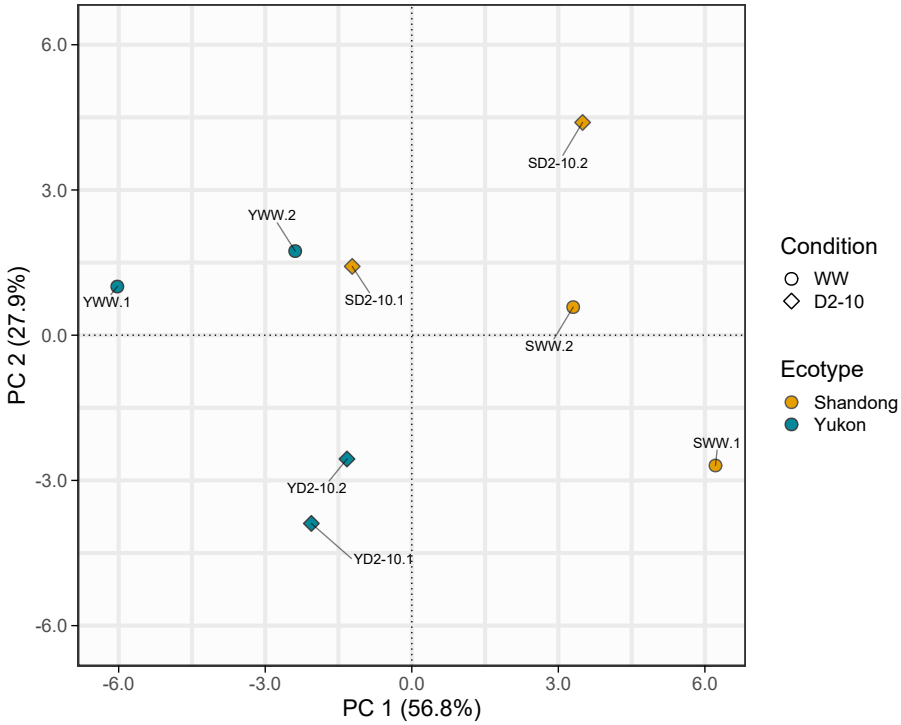

Figure 3.9: PC1 and PC2 biplot for SLA and OJIP fluorescence data for Yukon and Shandong *Eutrema* well-watered (WW) and D2-10 plants. (2 replicates, n=6)

A final comparison was performed using only OJIP data but including measurements from all stages of the progressive drought protocol and is shown in the biplot of Figure 3.10. Essentially, OJIP data do separate the ecotypes along PC1 with Yukon scores negative and Shandong scores positive to the origin. There seems to be no obvious pattern of scores related to treatment or recovery along PC2 for either ecotype. Figure 3.10 suggests that screening RILs for ecotype-specific drought responsive traits will benefit from comparisons between specific stages (eg. WW vs RW as seen in Figure 3.2(c)) which could greatly simplify a screening strategy for RILs going forward.

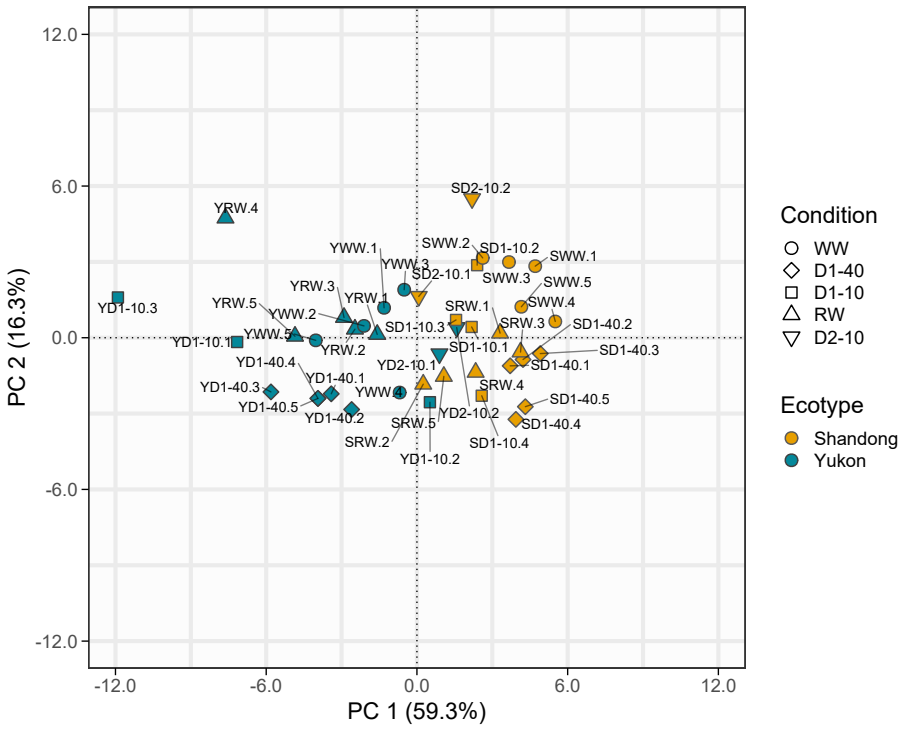

Figure 3.10: PCA biplot of OJIP fluorescence data corresponding to Yukon and Shandong plants at WW, D1-40, D1-10, RW (5 replicates, n=10), and D2-10 (3 replicates, n=10).

Table 3.6: First six Principal Component factor loadings for OJIP data at WW, D1-40, D1-10, RW, and D2-10 Shandong and Yukon plants.

	PC1	PC2	PC3	PC4	PC5	PC6
ϕ_{D_O}	-0.247	-0.028	0.047	-0.048	0.007	0.004
M_O	-0.241	-0.061	-0.086	-0.064	-0.002	0.146
$DI_O \cdot RC^{-1}$	-0.232	-0.137	0.104	-0.064	0.003	0.005
V_J	-0.209	0.149	-0.233	-0.018	-0.011	0.154
V_I	-0.204	0.079	-0.130	-0.033	-0.002	-0.722
F_O	-0.195	-0.252	-0.121	-0.137	-0.020	0.045
$ABS \cdot RC^{-1}$	-0.181	-0.277	0.179	-0.091	0.007	0.031
$TR_O \cdot RC^{-1}$	-0.128	-0.351	0.215	-0.102	0.010	0.047
$\phi_{P_{av}}$	-0.120	0.132	-0.004	-0.444	-0.200	-0.259
F_J	-0.110	-0.096	-0.451	-0.107	-0.026	0.209
F_I	0.041	-0.283	-0.371	-0.139	-0.036	-0.428
N	0.085	0.117	0.196	-0.547	-0.048	0.091
$TR_O \cdot RC^{-1}$	0.126	-0.297	0.313	-0.037	0.013	-0.109
S_M	0.127	0.255	0.075	-0.433	-0.070	0.066
S_S	0.129	0.346	-0.216	0.110	-0.034	-0.094
Fixed Area	0.165	-0.278	-0.231	-0.108	-0.022	0.067
F_M	0.169	-0.273	-0.228	-0.107	-0.015	0.088
Area	0.192	0.123	-0.016	-0.383	-0.056	0.097
HACH Area	0.207	-0.199	-0.188	-0.067	-0.016	0.052
F_V	0.209	-0.196	-0.185	-0.067	-0.009	0.072
ψ_O	0.209	-0.149	0.233	0.018	0.011	-0.154
ϕ_{E_O}	0.222	-0.126	0.192	0.019	0.006	-0.134
$\pi_{P_{Abs}}$	0.236	-0.032	0.080	0.033	-0.030	-0.166
$F_M \cdot F_O$	0.246	0.038	-0.051	0.051	-0.006	-0.009
$F_V \cdot F_O$	0.246	0.038	-0.051	0.051	-0.006	-0.009
$F_V \cdot F_M$	0.247	0.028	-0.047	0.048	-0.007	-0.004
ϕ_{P_O}	0.247	0.028	-0.047	0.048	-0.007	-0.004

Table 3.7: Average PSII quantum yield ($\phi PSII$) for Shandong and Yukon plants subjected to progressive drought protocols.

Eutrema salsugineum Ecotype	Treatment Stage $\phi PSII(Fv/Fm \pm SE)$				
	WW[a]	D1-40[a]	D1-10[a]	RW[a]	D2-10[b]
Shandong	0.816 ± 0.003	0.822 ± 0.001	0.811 ± 0.002	0.813 ± 0.002	0.816 ± 0.003
Yukon	0.789 ± 0.005	0.784 ± 0.005	0.784 ± 0.015	0.770 ± 0.010	0.811 ± 0.000

[a] Five replicates per genotype, n=20

[b] Three replicates per genotype, n=10

Average ϕ PS II ($F_V \cdot F_M^{-1}$) values were compared between Yukon and Shandong plants undergoing the progressive drought protocol (Table 3.7). In general, both ecotypes displayed similar values between unstressed (WW) and stressed conditions (D1-10, D1-40, RW, and D2-10) which suggests that the efficiency of PSII is unimpaired by the water deficit treatment we used. Although only two replicates were available, the higher $F_V \cdot F_M^{-1}$ value for Yukon plants at D2-10 relative to the other stages suggest the quantum efficiency of PSII could even be slightly improved by water deficits experienced by Yukon plants.

3.5 Screening recombinant inbred lines

At the RW stage of the successive drought treatment, Yukon but not Shandong plants, showed a significantly increased SLA (Figure 3.8) and this distinction was used to screen RILs. Figure 3.11 shows that some RILs resembled Shandong plants in displaying no significant differences in SLA values between WW and RW conditions (for examples see YS74#1, YS79#1, YS48#2, YS125#1, and YS15#2) although mean values for some RILs could be the same (YS79#1) or even higher (YS122#3) relative to SLA measurements for Shandong plants. Conversely, some RILs showed SLA values and RW-related differences in those measures in a manner resembling Yukon WW and RW plants. RILs with differences in SLA values comparable to those displayed by Yukon plants included YS98#3 and YS92#1 but the magnitude of these differences varied with the greatest one seen between WW and RW plants for RIL YS20#1. Finally, in at least one line the SLA for RW plants was smaller than for WW plants (ad63#5) which suggests that those plants likely did not grow or even regain full turgor after being re-watered. Figure 3.11 demonstrates that there is phenotypic diversity among the RILs with respect to SLA comparisons between the WW and RW stages of the drought treatment and in this regard, several lines undergo changes that are statistically significant.

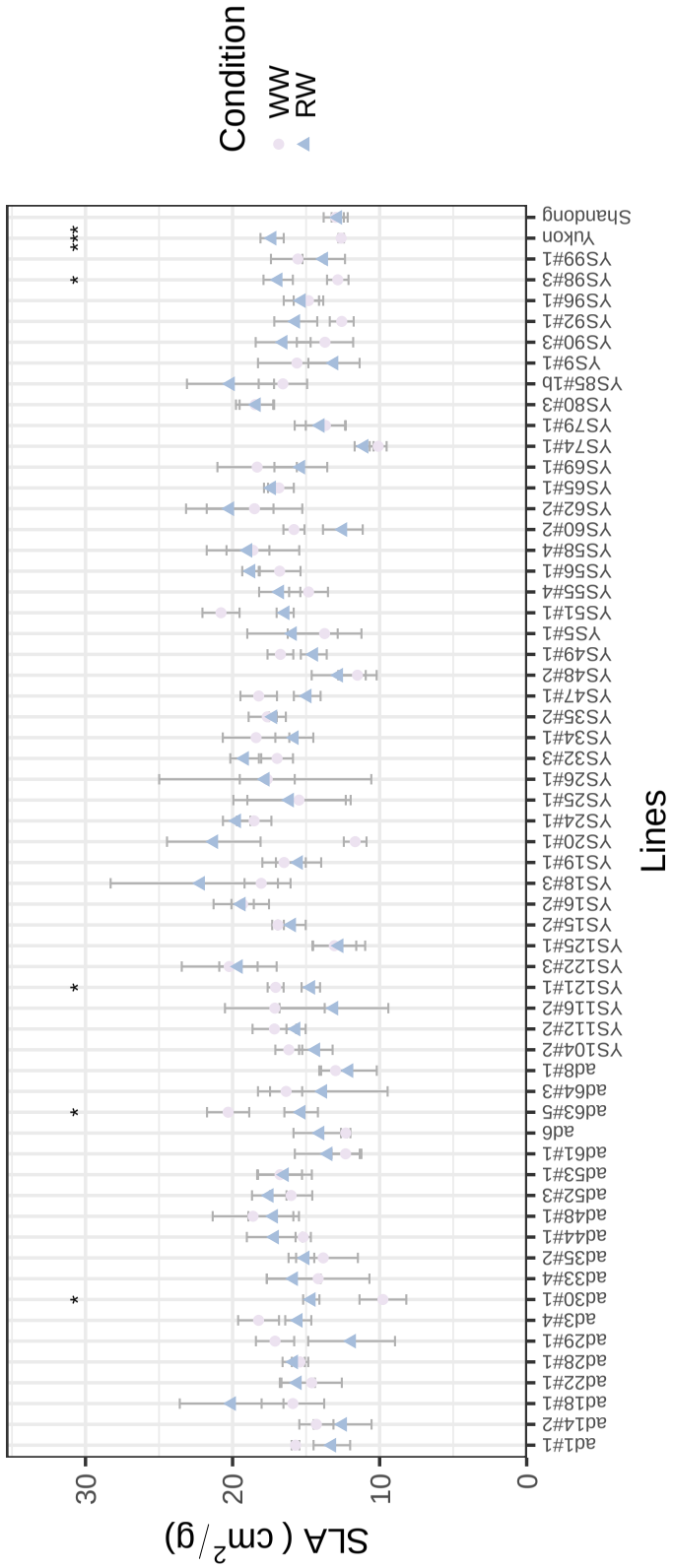

Figure 3.11: Summary of SLA data for RILs compared to Yukon and Shandong plants at the RW stage of progressive drought protocol. Significance is indicated as: single asterisk (*) $p < 0.05$ and triple asterisk (***) $p < 0.001$. Bars represent ± SEM (n=6).

A PCA biplot was used to visualize patterns between the two ecotypes and the range of different phenotypes with respect to OJIP data measured for the RILs (Figure 3.12). The first two PCs explain about 71% of the variation with PC1 distinguishing scores for Yukon plants positive along the x-axis and Shandong plants negative to the origin on the same axis. The biological significance of PC2 is less clear as symbols for RW and WW plants show no clear pattern. For PC1 the majority of RILs fall between the scores for Yukon in Shandong lines with some notable outliers including YS26#1RW, YS123#1RW, and YS24#1WW suggesting that they are differentially impacted by drought exposure than the other genotypes. The factors contributing to the positive direction along PC1 includes ϕ_{D_O}, M_O, and V_J (Table 3.8). Of note, the outlier RILs in Figure 3.12 were not found to have significantly different SLA measurements (Figure 3.11).

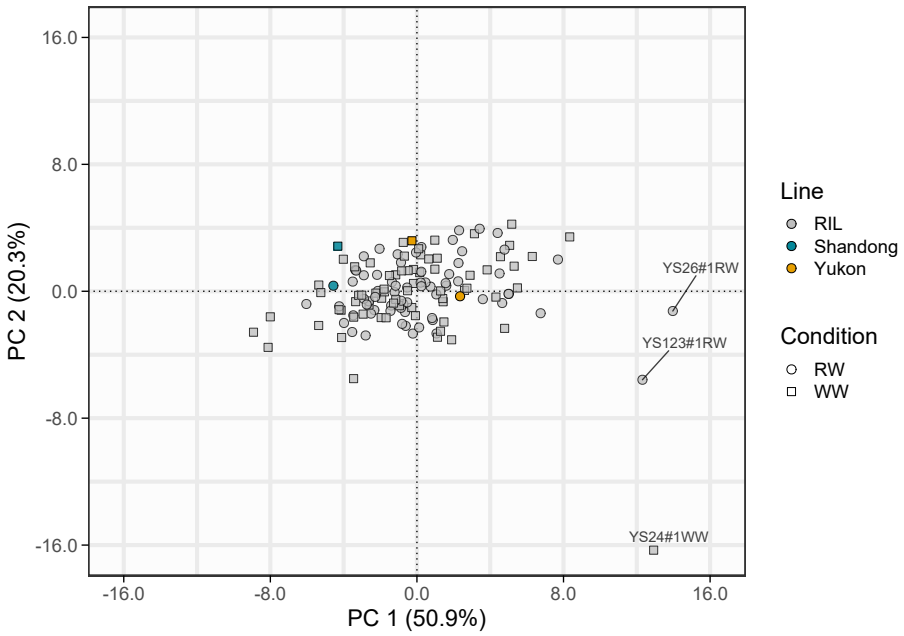

Figure 3.12: PCA biplot of OJIP fluorescence in RILs compared to RW and WW Yukon and Shandong lines (n=6).

Table 3.8: First six Principal Component factor loadings for RILs at RW and WW using OJIP data corresponding to biplot of Figure 3.12.

	PC1	PC2	PC3	PC4	PC5	PC6
$F_M \cdot F_O$	-0.262	-0.060	0.021	-0.088	0.017	-0.027
$F_V \cdot F_O$	-0.262	-0.060	0.021	-0.088	0.017	-0.027
ϕ_{P_o}	-0.261	0.049	-0.079	-0.042	-0.022	0.022
$F_V \cdot F_M$	-0.261	0.049	-0.079	-0.042	-0.024	0.024
ϕ_{E_o}	-0.247	-0.098	0.084	0.184	0.059	-0.043
π_{Abs}	-0.243	-0.129	0.030	0.020	0.116	-0.094
ψ_O	-0.233	-0.120	0.112	0.224	0.061	-0.049
F_V	-0.211	0.201	0.187	-0.127	-0.055	-0.039
HACH Area	-0.207	0.206	0.195	-0.125	-0.043	-0.024
$ET_O \cdot RC^{-1}$	-0.194	-0.066	0.213	0.357	0.062	0.062
F_M	-0.160	0.290	0.207	-0.119	-0.055	-0.039
Fixed Area	-0.154	0.294	0.214	-0.116	-0.043	-0.023
Area	-0.147	0.040	0.051	-0.279	0.592	0.345
S_S	-0.113	-0.166	-0.286	-0.383	-0.029	-0.325
F_I	-0.069	0.360	0.223	-0.017	0.056	-0.343
S_M	0.081	-0.270	0.336	-0.226	0.009	-0.038
N	0.086	-0.258	0.357	-0.196	-0.033	-0.052
$DI_O \cdot RC^{-1}$	0.110	-0.244	0.353	-0.165	-0.089	-0.092
F_J	0.114	0.339	0.049	-0.273	-0.115	0.027
$TR_O \cdot RC^{-1}$	0.119	0.144	0.298	0.382	0.041	0.302
$ABS \cdot RC^{-1}$	0.122	-0.217	0.379	-0.110	-0.081	-0.051
$\phi_{P_{av}}$	0.157	0.006	0.011	-0.119	0.698	0.008
F_O	0.173	0.311	0.075	0.025	-0.002	0.002
V_I	0.182	0.111	0.014	0.257	0.293	-0.707
V_J	0.233	0.120	-0.112	-0.224	-0.061	0.049
M_O	0.247	0.155	0.023	-0.041	-0.025	0.155
ϕ_{D_o}	0.261	-0.049	0.079	0.042	0.022	-0.022

$F_V \cdot F_M^{-1}$ was tested as a potential screening tool to distinguish WW from RW plants with results given in Figure 3.13. Relative of the five RILs showing significant differences on the basis of SLA (Figure 3.11), 18 RILs were identified as showing significant differences between RW and WW conditions using $F_V \cdot F_M^{-1}$ (ad3#4, ad33#4, ad48#1, ad6, YS123#1, YS20#1, YS26#1, and YS65#1). Suggesting that the impact of WW and RW conditions is differential on lines at the level of SLA versus fluorescence. This impression is further instilled by the finding that there is no overlap between RILs showing significant differences for both SLA (Figure 3.11) and $F_V \cdot F_M^{-1}$ (Figure 3.13). With respect to $F_V \cdot F_M^{-1}$, the lines generally showed higher values for quantum yield as WW relative to RW plants, but some interesting exceptions were found such as YS24#1 and YS20#1 which suggests a gain in efficiency relative to WW plants following recovery from drought. These tests should be repeated to confirm this pattern.

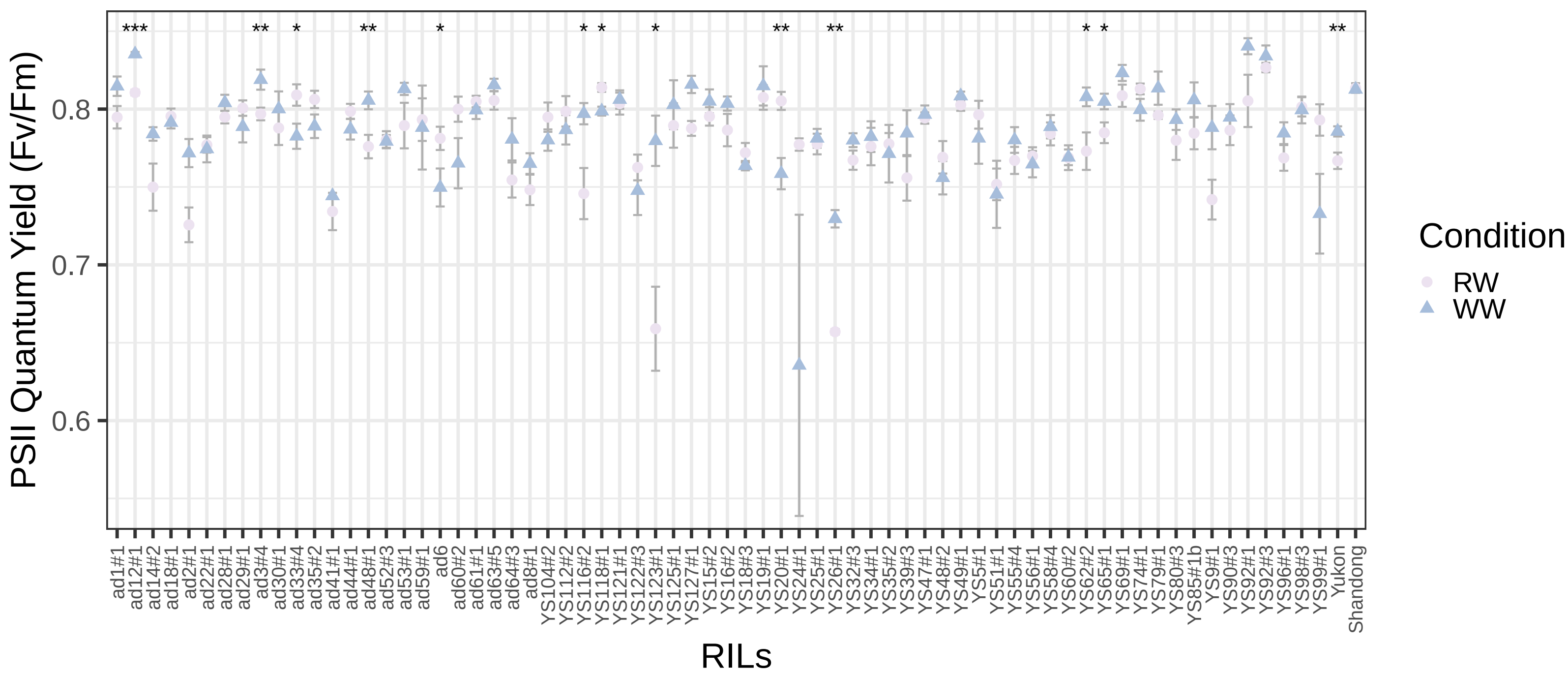

Figure 3.13: PSII Quantum Yield estimates for WW and RW RILs relative to Yukon and Shandong ecotypes. Survey of 68 independent RILs was performed. Significance is indicated as: * ($p < 0.05$), ** ($p < 0.01$), *** ($p < 0.001$), and **** ($p < 0.0001$). Bars represent ± SEM (n=6).

PSII quantum yield ($F_V \cdot F_M^{-1}$) measurements were plotted as a histogram to identify the range of measurements for the ecotypes and their RILs (Figure 3.14) and to identify outliers. Outliers could help identify RILs with greater or lesser tolerance to drought relative to the Shandong and Yukon lines. The average value for $F_V \cdot F_M^{-1}$ was 0.79 for WW RILs whereas 0.785 was the value determined for RW RILs, so there is considerable overlap in the two determinations indicating that WW and RW plants are very similar in this regard. However, two bars fell below 0.70 PSII efficiency represent data for three RILs, two for RW plants (YS 123#1 and YS26#1) and one for a WW plant (YS24#1) (Figure 3.13).

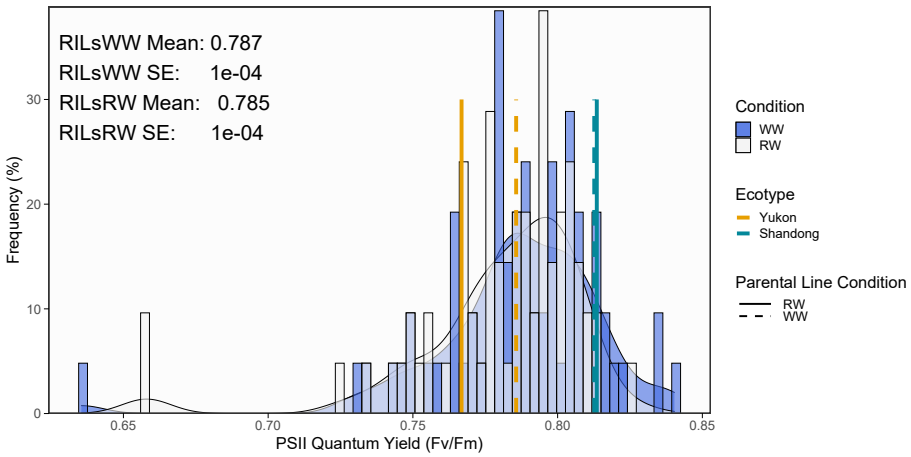

Figure 3.14: Histogram of PSII efficiency ($F_V \cdot F_M^{-1}$) estimates for RILs, Yukon, and Shandong lines at WW and RW stages of progressive drought treatment.

Chapter 4: Discussion

Eutrema salsugineum is an extremophyte capable of withstanding a number of abiotic stressors such as salt, drought, extreme cold, and phosphate deficiency, making it an excellent model plant for studying how plants cope with abiotic stress (Guevara et al., 2012; MacLeod et al., 2015; Velasco et al., 2016). Tolerance to stress, however, is a complex, multigenic trait, and hence identifying genes associated with coping mechanisms related to stress, particularly to drought stress, has been a challenge (review by Nuccio et al., 2018). Quantitative trait loci (QTL) analysis is a useful approach for identifying genes associated with complex traits like drought tolerance. The key to QTL analysis is evidence that one has at least two strains or genotypes with divergent, heritable traits, suggesting that genetic markers can be identified to enable QTL analysis. We began this work with the knowledge that Yukon and Shandong *Eutrema* ecotypes were divergent with respect to drought tolerance in that Yukon plants display better tolerance to water deficits whereas Shandong plants follow avoidance strategies (MacLeod et al., 2015). The phenotypic differences reported by MacLeod et al. (2015) for the two ecotypes undergoing a two-stage progressive drought treatment were barely discernible but recently those modest phenotypic changes were found to be associated with dramatic, differential remodeling of Yukon and Shandong *Eutrema* transcriptomes (Simopoulos et al., 2020). With over a thousand genes showing drought-responsive differential expression between the ecotypes, narrowing the field to fewer genes of interest, such as QTLs that show heritability with drought tolerance, takes on greater importance in providing a smaller number of gene leads meriting validation for their potential to improve crop tolerance to water deprivation.

In this work we used recombinant inbred lines (RILs), produced by crossing Yukon and Shandong plants, to develop and test a screening strategy to identify phenotypic and physiological markers for drought tolerance that could be used to screen the parent lines and their RILs under well-watered and water deficit treatments. The fact that the transcriptomes differ with exposure to a water deficit stress is encouraging especially with evidence that molecular markers are available (Simopoulos et al., 2020) and that QTL analysis could be a valuable approach for identifying genes contributing to drought tolerance. However, at the onset of this work we were uncertain about the

best phenotypic feature(s) that signal a beneficial, quantifiable response to drought exposure that also would provide a sufficiently clear distinction between the phenotypes of Yukon and Shandong plants experiencing drought and also was amenable for screening many RILs to test for heritability. Plants display many different responses when exposed to a water deficit however, not all are positively correlated to plant vigor after a drought stress. Moreover, traits that show a strong association with tolerance are not necessarily suitable for efficiently screening many plants. Ideally phenotypic screens should be non-invasive and non-destructive so that repetitive measurements can be made on the same plant allowing for evaluations on plant response and recovery to successive stress treatments. The measurements should also be amenable to high-confidence statistics without requiring unmanageable sampling levels. By way of example, the CRWL assay used in this study and by MacLeod et al. (2015) provides a reasonably good measure to differentiate water loss behaviour between Yukon and Shandong plants (Figure 3.1(a)), but the need to sever shoots from roots to perform this test precludes using the same plant for a continuation of measurements in response to the same or different stressors.

ln this study we took advantage of a progressive drought protocol that followed plants exposed to two successive drought treatments separated by a recovery stage (D1 $\rightarrow$ RW $\rightarrow$ D2). Sampling was carried out during the drought treatment and synchronized gravimetrically by determining pot weight to define the extent of a water deficit stress at prescribed stages: FTSW 40% (plants under relatively mild stress) or 10% (plants under a severe water deficit but not wilted) (MacLeod et al., 2015). Further, we predicted from the work of MacLeod et al. (2015) that Yukon, but not Shandong plants, would establish a heightened tolerance to drought during D1. The impact of that enhanced capacity would be expressed during the D2 stage of the protocol where Yukon plants would take more time (by day or two) to wilt and show a higher SLA measurement relative to Shandong plants at the same stage of treatment. This work largely focused on comparing phenotypes related to water use and photosynthesis between Yukon and Shandong plants during D1 to see if phenotypic screening was possible at this stage. This was followed up by seeing whether promising phenotypic traits between the ecotypes could be used to detect differential drought responses between RILs and whether evidence of a heritable pattern could be detected concerning tolerance (Yukon trait) or sensitivity (Shandong trait) to water deficits.

Multiple physiological measurements were taken among the D1-40, D1-10, RW, and D2-10 stages of drought (Figure 2.4) but not all traits were measured at every stage. As discussed above, there was an interest in focusing on D1 for phenotypic markers useful at this stage so more experimental replicates covered the first stage of drought. Some assays were more laborious and so were not performed at all of the drought stages shown in Figure 2.4. For example, anthocyanin content and cut rosette water loss (CRWL) assays were performed at D1-40, solute potential at D1-10, relative water content (RWC), static leaf water content (SLWC) were determined at RW, specific leaf area (SLA) at RW as well as D2-10. The FluorPen is a handheld device that made performing measurements of OJIP fluorescence simple and efficient so this device was used at all drought stages. Of the foregoing measurements, OJIP fluorescence emission and SLA determinations were found to be the best at differentiating between Shandong and Yukon plants (Figures 3.2 and 3.8). Furthermore, when applied to testing the RILs, OJIP and SLA data were able to distinguish between RILs. Outlying RILs were reproducibly positioned away from a central grouping of RILs with intermediate performance in respect to these traits (Figures 3.12 and 3.14).

For the methods used in this thesis and also by MacLeod et al. (2015), the findings are in agreement. Where there was overlap in the data we both found the *Eutrema salsugineum* ecotypes to either display similar or slightly different responses to drought. Contrasting responses between the ecotypes were observed during D1-40 for anthocyanin content with significantly higher CRWL value for Shandong relative to Yukon plants and a significantly higher anthocyanin level only found for drought-stressed Yukon plants (Figure 3.1). At a more severe water deficit, D1-10, evidence for solute accumulation was detected in Yukon plants but not Shandong plants (Figure 3.4). At RW, both ecotypes displayed similar recovery values for RWC and SLWC (Figure 3.6). However, at RW significant differences were found in chlorophyll fluorescence (Figure 3.2(c)) and leaf area expansion (Figure 3.8(a)) which together likely contribute to separation seen in the PCA biplot of Figure 3.7 where RW Yukon plants (YRW) clearly clustered to the left of the origin and away from positive scores corresponding to RW Shandong plants (SRW).

Changes in chlorophyll fluorescence also distinguished the response between the ecotypes at D2-10. This differential response is shown in the position of the scores in a PCA for OJIP data alone (Figure 3.2(d), Figure 3.10) or when OJIP data was combined with SLA measurements (Figure 3.9). With a focus on components of

OJIP data, Table 3.2 shows that the ecotypes do not overlap with respect to Fv/Fm values, measures of PSII efficiency, rather that Yukon plants tend to have a lower baseline value relative to Shandong plants although it is a minor difference that is largely removed at D2-10 when the average Fv/Fm value in Yukon plants of 0.77 and 0.81 at D2-10 (Table 3.7). Relative to accepted ranges in the literature, it seems neither ecotype is showing a significant drop in PSII efficiency, at least not one that is captured by the Fv/Fm ratio which is considered to typically fall between 0.78 and 0.85 for unstressed plants (Guidi et al., 2019) and Table 3.7 has no ratios that fall markedly below this range, even when plants are in pots with little to no water (D1-10 or D2-10). A drop in PSII efficiency would be consistent with stress adversely impacting photosynthesis but its use alone is not always regarded as a reliable measure of stress (Maxwell and Johnson, 2000; Guidi et al., 2019).

Interestingly, values of Fv/Fm for the Shandong ecotype were slightly higher relative to those of Yukon plants with Fv/Fm values between 0.81-0.82 and 0.77-0.81 for Shandong and Yukon plants, respectively (Table 3.7). The distinction is nominal and would be in keeping with the conclusion of Khanal et al. (2017) that the *Eutrema* ecotypes both show resilient mechanisms to protect PSII, even when exposed to cold temperatures. It would seem that both ecotypes are also resilient to drought in that Fv/Fm values at D2-10 resemble those of unstressed plants (WW), even when 90% of the transpirable soil water is gone. This also suggests that the use of a decrease in the Fv/Fm, advocated as one type of stress imaging tool (Lichtenthaler et al., 2005), would not be a useful drought screen for QTL-analysis. While the ratio of Fv/Fm may not distinguish the RILs, the components used to derive this ratio could be helpful in discerning differences between the ecotypes (Table 3.7). F_V describes the variable range of fluorescence, the difference between maximal fluorescence and the dark-adapted condition (F_M-F_O) (Hermans et al., 2003). As a screen, only the comparison made between Shandong RW and WW plants showed any difference for F_O, F_M or F_V values and no differences are seen for either ecotype with respect to these measurements at the most severe, D2-10 treatment stage.

An interesting, and perhaps relevant observation, on the relationship between stress and photosynthesis was reported by Khanal et al. (2017) in their comparison between both *Eutrema* ecotypes used here and *Arabidopsis* with plants grown at in the presence or absence of low temperature stress and at variable light levels. The authors found evidence for differential cold acclimation between these genotypes and

varying the light conditions had a differential effect on their capacity to acclimate to cold temperatures. Interestingly, use of low light levels typically used to grow *Arabidopsis*, when applied to all three genotypes, led to impaired growth for Yukon but not Shandong plants as determined by light response curves. Specifically, the authors noted that no light response data could be collected for Yukon *Eutrema* when plants were grown under consistent *Arabidopsis* conditions because the plants failed to thrive. Khanal et al. (2017) also performed many of their photosynthetic measurements using plants grown under light, daylength, and temperature conditions similar to ours, and for those plants they found *Arabidopsis* Fv/Fm values ranging between 0.82 to 0.83, values for Shandong plants between 0.81 to 0.84 and those for Yukon plants around 0.79 to 0.82, the latter *Eutrema* values in good agreement with the values for those ecotypes reported in this thesis (Table 3.7; Khanal et al., 2017).

The work of Khanal et al. (2017) raises a question about growth conditions and a possible plasticity in photosynthetic processes when a plant is exposed to stress. What our work does not consider is whether altering light levels used during the growth of our plants could impact how the plants respond to drought and whether this factor should probably be tested in that regard. Would, for example, the robust drought tolerance shown by Yukon *Eutrema* under our conditions be attenuated under lower light levels? In a recent study comparing *Arabidopsis thaliana* with Shandong *Eutrema*, the authors concluded that *A. thaliana*, *A. lyrata*, and *Eutrema* may differ in their signaling response pathways related to drought, but differences in their response to drought were deemed modest, even between the extremophyte *Eutrema* and the comparatively drought sensitive *A. thaliana* (Rosa et al., 2019). It is notable that their study used light levels of 110 to 120 μmol $m^{-2}s^{-1}$ which would be the low and problematic light intensity level identified by Khanal et al. (2017) in their study on cold tolerance. Clearly there are differences in growth conditions used by various labs studying *Eutrema* and identifying environmental conditions that amplify or suppress the drought responses observed in *Eutrema* could resolve contradictory findings that may be emerging as interest in this species as a model for stress tolerance increases. This would be one avenue for future research with respect to drought responses of *Eutrema*. On the matter of light intensity, high light may not be deleterious, even under severe field conditions. An average Fv/Fm of 0.7 was found for field plants at Yukon sites where saturating light levels of around 1500 to 2000 μmol $m^{-2}s^{-1}$ are found (Peter Summers, unpublished). Field measurements are notoriously difficult to

take reliably, as establishing a value for F_O is difficult under field conditions (Murchie and Lawson, 2013; Maxwell and Johnson, 2000). With this caveat in mind, the average Fv/Fm value for Yukon field plants is only about 13% less than the average Fv/Fm value for plants in growth cabinets and that is in spite of plants in the field growing on highly saline soil that had received little to no recent precipitation. Testing variable light levels systematically in growth cabinets under controlled light and temperature conditions would help determine whether the light intensity under which plants have grown can alter OJIP measurements and hence alter our interpretation of drought tolerance behaviour for these ecotypes. In pragmatic terms, using PSII efficiency as a means of screening RILs could be problematic if the drought response that distinguishes the parental lines is "plastic" and influenced by other environmental conditions aside from water availability.

Despite PSII efficiency being used as a common measurement for abiotic stress in plants, lending itself to be simple, non-destructive, allowing quick replicate measurements, future work with the RILs may benefit from further investigation into a second drought exposure and inclusive of other fluorescent measurements. Comparing PCAs of OJIP fluorescence data at different stages of drought was helpful in determining which stage bests separates the ecotypes with RW displaying the earliest separation between treatments for the Yukon ecotype (Figure 3.2). At this stage of drought few RILs are distinguished from the others at edge of the PSII histogram and similar results are seen with OJIP fluorescence as given only three notable RIL outliers: YS24#1, YS26#1, and YS123#1 (Figures 3.12 and 3.14). However, there was no overlap between RILs identified as outliers using Fv/Fm and outliers identified by SLA (Figures 3.11 and 3.13). Marcos et al. (2018) found that sugarcane (*Saccharum* spp.) plants displayed better water use efficiency and photosynthetic performance after a second and then third water water deficit compared to a first exposure. This was reflective of my findings with many differences found between Shandong and Yukon plants not only at RW but also at a second exposure (D2-10) (Table 3.7 and Figure 3.9). Following an initial water deficit, Citrus x limona (Rangpur Lime and Sunki Maravilha) plants are more tolerant of subsequent water deficits with increases in stomatal conductance, photosynthetic rates, and transpiration (Neves et al., 2017). Neves et al. (2017) also found evidence of epigenetic influences supported by a "stress memory" that correlated with altered hormone levels (increased abscisic acid (ABA) and indole acetic acid (IAA) content), and evidence of DNA methylation in response

to successive drought exposures. This suggests that some of our RILs having subtly different traits from the parental lines could still display contrasting expression relative to ecotypes or be products of epigenetic changes. Subtle differences between the ecotypes in a first drought exposure could become more remarkable after a second water deficit, perhaps even a third, for future screening of RILs.

To conclude, *Eutrema salsugineum* is an extremophyte that displays a complex coping response towards stress influenced by factors such as light intensity (Khanal et al., 2017) or a single water deficit exposure (Griffith et al., 2007; MacLeod et al., 2015). The interactions between environmental conditions and stress tolerance presents a challenge towards finding an easy, reliable screen for a drought tolerance between the ecotypes or among their RILs. The drought-priming response shown by Yukon plants leading to a better tolerance towards water deficit is not unique to this genotype as it has been identified for sugarcane (Marcos et al., 2018) and even associated with epigenetic regulation for citrus (Neves et al., 2017). As a consequence, this response may be more general and one that would be useful towards crop improvement. However there may also be an opportunity to use multiple drought treatments in succession to not only screen for drought tolerance but also the capacity for plants to recover from drought. Little information is available that tells us whether strong and positive recovery from drought is necessarily linked to tolerance toward this stressor. Future research using Eutrema ecotypes and RILs could use successive drought treatments to help identify the genetic determinants of drought tolerance and drought recovery in the extent to which these processes overlap. Our crops must not only endure drought; they must be able to remain productive following recovery to ensure food security in the face of climate change.

References

Abràmoff, M. D., P. J. Magalhães, and S. J. Ram (2004). "Image processing with ImageJ". *Biophotonics International* 11.7, pp. 36–42.

Amtmann, A. (2009). "Learning from Evolution: *Thellungiella* Generates New Knowledge on Essential and Critical Components of Abiotic Stress Tolerance in Plants". *Molecular Plant* 2.1, pp. 3–12.

Baerenfaller, K., C. Massonnet, S. Walsh, S. Baginsky, P. Bühlmann, L. Hennig, M. Hirsch-Hoffmann, K. A. Howell, S. Kahlau, A. Radziejwoski, D. Russenberger, D. Rutishauser, I. Small, D. Stekhoven, R. Sulpice, J. Svozil, N. Wuyts, M. Stitt, P. Hilson, C. Granier, and W. Gruissem (2012). "Systems-based analysis of Arabidopsis leaf growth reveals adaptation to water deficit". *Molecular Systems Biology* 8.1.

Boyer, J. S. (1982). "Plant productivity and environment". *Science* 218.4571, pp. 443–448.

Brodribb, T. J. and H. Cochard (2009). "Hydraulic failure defines the recovery and point of death in water-stressed conifers". *Plant Physiology* 149.1, pp. 575–584.

Choat, B., S. Jansen, T. J. Brodribb, H. Cochard, S. Delzon, R. Bhaskar, S. J. Bucci, T. S. Feild, S. M. Gleason, U. Hacke, A. Jacobsen, F. Lens, H. Maherali, J. Martínez-Vilalta, S. Mayr, M. Mencuccini, M. Patrick, A. Nardini, J. Pittermann, B. Pratt, J. Sperry, M. Westoby, I. Wright, and A. Zanne (2012). "Global convergence in the vulnerability of forests to drought". *Nature* 491.7426, p. 752.

Cuneo, I. F., T. Knipfer, C. R. Brodersen, and A. J. McElrone (2016). "Mechanical failure of fine root cortical cells initiates plant hydraulic decline during drought". *Plant Physiology* 172.3, pp. 1669–1678.

FAO, IFAD, UNICEF, WFP, and WHO (2017). "The State of Food Security and Nutrition in the World". *Building reslience for peace and food security. Rome, FAO*.

Flexas, J and H Medrano (2002). "Drought-inhibition of photosynthesis in C3 plants: stomatal and non-stomatal limitations revisited". *Annals of Botany* 89.2, pp. 183–189.

Gadjev, I., S. Vanderauwera, T. S. Gechev, C. Laloi, I. N. Minkov, V. Shulaev, K. Apel, D. Inzé, R. Mittler, and F. Van Breusegem (2006). "Transcriptomic foot-

prints disclose specificity of reactive oxygen species signaling in Arabidopsis". *Plant Physiology* 141.2, pp. 436–445.

Griffith, M., M. Timonin, A. C. Wong, G. R. Gray, S. R. Akhter, M. Saldanha, M. A. Rogers, E. A. Weretilnyk, and B. Moffatt (2007). "Thellungiella: an Arabidopsis-related model plant adapted to cold temperatures". *Plant, Cell & Environment* 30.5, pp. 529–538.

Guevara, D. R., M. J. Champigny, A. Tattersall, J. Dedrick, C. E. Wong, Y. Li, A. Labbe, C.-L. Ping, Y. Wang, P. Nuin, B. G. Golding, B. E. McCarry, P. S. Summers, B. A. Moffatt, and E. Weretilnyk (2012). "Transcriptomic and metabolomic analysis of Yukon *Thellungiella* plants grown in cabinets and their natural habitat show phenotypic plasticity". *BMC Plant Biology* 12.1, p. 175.

Guidi, L., E. Lo Piccolo, and M. Landi (2019). "Chlorophyll Fluorescence, Photoinhibition and Abiotic Stress: Does it Make Any Difference the Fact to Be a C3 or C4 Species?" *Frontiers in Plant Science* 10, p. 174.

Hahlbrock, K. and D. Scheel (1989). "Physiology and molecular biology of phenylpropanoid metabolism". *Annual Review of Plant Biology* 40.1, pp. 347–369.

Hermans, C., M. Smeyers, R. M. Rodriguez, M. Eyletters, R. J. Strasser, and J.-P. Delhaye (2003). "Quality assessment of urban trees: a comparative study of physiological characterisation, airborne imaging and on site fluorescence monitoring by the OJIP-test". *Journal of Plant Physiology* 160.1, pp. 81–90.

Hsiao, T. C., E Acevedo, E Fereres, and D. Henderson (1976). "Water stress, growth and osmotic adjustment". *Philosophical Transactions of the Royal Society of London. B, Biological Sciences* 273.927, pp. 479–500.

Hughes, J., C. Hepworth, C. Dutton, J. A. Dunn, L. Hunt, J. Stephens, R. Waugh, D. D. Cameron, and J. E. Gray (2017). "Reducing stomatal density in barley improves drought tolerance without impacting on yield". *Plant Physiology* 174.2, pp. 776–787.

Jones, M. M. and N. C. Turner (1978). "Osmotic adjustment in leaves of sorghum in response to water deficits". *Plant Physiology* 61.1, pp. 122–126.

Jones, M., N. Turner, and C. Osmond (1980). "Accumulation of solutes in leaves of sorghum and sunflower in response to water deficits". *Functional Plant Biology* 7.2, pp. 193–205.

Kalaji, H. M., G. Schansker, M. Brestic, F. Bussotti, A. Calatayud, L. Ferroni, V. Goltsev, L. Guidi, A. Jajoo, P. Li, P. Losciale, V. Mishra, A. Misra, S. Nebauer,

S. Pancaldi, C. Penella, M. Pollastrini, K. Suresh, E. Tambussi, M. Yanniccari, M. Zivcak, M. Cetner, I. Samborska, A. Stirbet, K. Olsovska, K. Kunderlikova, H. Shelonzek, S. Rusinowski, and W. Bąba (2017). "Frequently asked questions about chlorophyll fluorescence the sequel". *Photosynthesis Research* 132.1, pp. 13–66.

Kalaji, H. M., G. Schansker, R. J. Ladle, V. Goltsev, K. Bosa, S. I. Allakhverdiev, M. Brestic, F. Bussotti, A. Calatayud, P. Dąbrowski, et al. (2014). "Frequently asked questions about in vivo chlorophyll fluorescence: practical issues". *Photosynthesis research* 122.2, pp. 121–158.

Kautsky, H. and A. Hirsch (1931). "Neue Versuche Zur Kohlensäureassimilation". *Naturwissenschaften* 19.48, pp. 964–964.

Kazachkova, Y., A. Batushansky, A. Cisneros, N. Tel-Zur, A. Fait, and S. Barak (2013). "Growth Platform-Dependent and -Independent Phenotypic and Metabolic Responses of Arabidopsis and Its Halophytic Relative, *Eutrema salsugineum*, to Salt Stress". *Plant Physiology* 162.3, pp. 1583–1598.

Khanal, N., G. E. Bray, A. Grisnich, B. A. Moffatt, and G. R. Gray (2017). "Differential mechanisms of photosynthetic acclimation to light and low temperature in *Arabidopsis* and the extremophile *Eutrema salsugineum*". *Plants* 6.3, p. 32.

Kim, J., H. Yi, G. Choi, B. Shin, P.-S. Song, and G. Choi (2003). "Functional characterization of phytochrome interacting factor 3 in phytochrome-mediated light signal transduction". *The Plant Cell* 15.10, pp. 2399–2407.

Kovinich, N., G. Kayanja, A. Chanoca, M. S. Otegui, and E. Grotewold (2015). "Abiotic stresses induce different localizations of anthocyanins in *Arabidopsis*". *Plant Signaling & Behavior* 10.7, e10278501–e10278504.

LMC International (2016). *The Economic Impact of Canola on the Canadian Economy*. Tech. rep.

Lang, J., M. Barták, J. Hájek, P. Váczi, and B. Zikmundová (2020). "Chilling effects on primary photosynthetic processes in *Medicago sativa*: Acclimatory changes after short-and long-term exposure to low temperatures". *Biologia*, pp. 1–10.

Lichtenthaler, H., C Buschmann, and M Knapp (2005). "How to correctly determine the different chlorophyll fluorescence parameters and the chlorophyll fluorescence decrease ratio R_{Fd} of leaves with the PAM fluorometer". *Photosynthetica* 43.3, pp. 379–393.

Loggini, B., A. Scartazza, E. Brugnoli, and F. Navari-Izzo (1999). "Antioxidative defense system, pigment composition, and photosynthetic efficiency in two wheat cultivars subjected to drought". *Plant Physiology* 119.3, pp. 1091–1100.

MacLeod, M. J., J. Dedrick, C. Ashton, W. W. Sung, M. J. Champigny, and E. A. Weretilnyk (2015). "Exposure of two *Eutrema salsugineum* (*Thellungiella salsuginea*) accessions to water deficits reveals different coping strategies in response to drought". *Physiologia Plantarum* 155.3, pp. 267–280.

Marcos, F. C., N. M. Silveira, J. B. Mokochinski, A. C. Sawaya, P. E. Marchiori, E. C. Machado, G. M. Souza, M. G. Landell, and R. V. Ribeiro (2018). "Drought tolerance of sugarcane is improved by previous exposure to water deficit". *Journal of Plant Physiology* 223, pp. 9–18.

Maxwell, K. and G. N. Johnson (2000). "Chlorophyll fluorescence—a practical guide". *Journal of Experimental Botany* 51.345, pp. 659–668.

Miklas, P. N., W. C. Johnson, R. Delorme, and P. Gepts (2001). "QTL conditioning physiological resistance and avoidance to white mold in dry bean". *Crop Science* 41.2, pp. 309–315.

Morgan, J. (1980). "Osmotic adjustment in the spikelets and leaves of wheat". *Journal of Experimental Botany* 31.2, pp. 655–665.

Murchie, E. H. and T. Lawson (2013). "Chlorophyll fluorescence analysis: a guide to good practice and understanding some new applications". *Journal of Experimental Botany* 64.13, pp. 3983–3998.

Neves, D. M., L. A. da Hora Almeida, D. D. S. Santana-Vieira, L. Freschi, C. F. Ferreira, W. dos Santos Soares Filho, M. G. C. Costa, F. Micheli, M. A. Coelho Filho, and A. da Silva Gesteira (2017). "Recurrent water deficit causes epigenetic and hormonal changes in citrus plants". *Scientific Reports* 7.1, pp. 1–11.

Nuccio, M. L., M. Paul, N. J. Bate, J. Cohn, and S. R. Cutler (2018). "Where are the drought tolerant crops? An assessment of more than two decades of plant biotechnology effort in crop improvement". *Plant Science* 273, pp. 110–119.

Oukarroum, A., G. Schansker, and R. J. Strasser (2009). "Drought stress effects on photosystem I content and photosystem II thermotolerance analyzed using Chl *a* fluorescence kinetics in barley varieties differing in their drought tolerance". *Physiologia Plantarum* 137.2, pp. 188–199.

Papageorgiou, G. et al. (1975). "Chlorophyll fluorescence: an intrinsic probe of photosynthesis". *Bioenergetics of Photosynthesis*, pp. 319–371.

Pollard, D. A. (2012). "Design and construction of recombinant inbred lines". In: *Quantitative Trait Loci (QTL)*. Springer, pp. 31–39.

QGIS Team, D. (2016). "QGIS Geographic Information System". *Open source geospatial foundation project*.

RStudio Team (2020). *RStudio: Integrated Development Environment for R*. RStudio, PBC. Boston, MA.

Rosa, N. Marín-de la, C.-W. Lin, Y. J. Kang, S. Dhondt, N. Gonzalez, D. Inzé, and P. Falter-Braun (2019). "Drought resistance is mediated by divergent strategies in closely related Brassicaceae". *New Phytologist* 223.2, pp. 783–797.

Simopoulos, C. M., M. J. MacLeod, S. Irani, W. W. Sung, M. J. Champigny, P. S. Summers, G. B. Golding, and E. A. Weretilnyk (2020). "Coding and long non-coding RNAs provide evidence of distinct transcriptional reprogramming for two ecotypes of the extremophile plant *Eutrema salsugineum* undergoing water deficit stress". *BMC Genomics* 21.1, pp. 1–16.

Smirnoff, N. (1993). "The role of active oxygen in the response of plants to water deficit and desiccation". *The New Phytologist* 125.1, pp. 27–58.

Stirbet, A. and Govindjee (2011). "On the relation between the Kautsky effect (chlorophyll a fluorescence induction) and Photosystem II: Basics and applications of the OJIP fluorescence transient". *Journal of Photochemistry and Photobiology B: Biology* 104, pp. 236–257.

Strasser, R. J. and Govindjee (1992). "The Fo and the O-J-I-P fluorescence rise in higher plants and algae". In: *Regulation of Chloroplast Biogenesis*. Springer, pp. 423–426.

Strasser, R. J., M. Tsimilli-Michael, and A. Srivastava (2004). "Analysis of the chlorophyll a fluorescence transient". In: *Chlorophyll a fluorescence*. Springer, pp. 321–362.

Strasser, R. J., A. Srivastava, and M Tsimilli-Michael (2000). "The fluorescence transient as a tool to characterize and screen photosynthetic samples". *Probing Photosynthesis: Mechanisms, Regulation and Adaptation*, pp. 445–483.

Sunil, B, R. Strasser, and A. Ragavendra (2020). "Special issue in honour of Prof. Reto J. Strasser–Targets of nitric oxide (NO) during modulation of photosystems in pea mesophyll protoplasts: studies using chlorophyll a fluorescence". *Photosynthetica* 58.Special Issue, pp. 452–459.

Telfer, A., S. M. Bishop, D. Phillips, and J. Barber (1994). "Isolated Photosynthetic reaction center of photosystem II as a sensitizer for the formation of singlet oxygen. Detection and quantum yield determination using a chemical trapping technique." *Journal of Biological Chemistry* 269.18, pp. 13244–13253.

Van Eerden, F. J., M. N. Melo, P. W. Frederix, X. Periole, and S. J. Marrink (2017). "Exchange pathways of plastoquinone and plastoquinol in the photosystem II complex". *Nature Communications* 8, p. 15214.

Velasco, V. M. E., J. Mansbridge, S. Bremner, K. Carruthers, P. S. Summers, W. W. Sung, M. J. Champigny, and E. A. Weretilnyk (2016). "Acclimation of the crucifer *Eutrema salsugineum* to phosphate limitation is associated with constitutively high expression of phosphate-starvation genes". *Plant, Cell & Environment* 39.8, pp. 1818–1834.

Weretilnyk, E. A., D. D. Smith, G. A. Wilch, and P. S. Summers (1995). "Enzymes of Choline Synthesis in Spinach". *Plant Physiology* 109.3, pp. 1085–1091.

Yue, B., W. Xue, L. Xiong, X. Yu, L. Luo, K. Cui, D. Jin, Y. Xing, and Q. Zhang (2006). "Genetic basis of drought resistance at reproductive stage in rice: separation of drought tolerance from drought avoidance". *Genetics* 172.2, pp. 1213–1228.

Zhang, F.-P. and T. J. Brodribb (2017). "Are flowers vulnerable to xylem cavitation during drought?" *Proceedings of the Royal Society B: Biological Sciences* 284.1854, pp. 1–8.

Zhao, X., B. Feng, T. Chen, C. Zhang, L. Tao, and G. Fu (2017). "Transcriptome analysis of pale-green leaf rice reveals photosynthetic regulatory pathways". *Acta Physiologiae Plantarum* 39.12, pp. 274–282.

Zlatev, Z. S. and I. T. Yordanov (2004). "Effects of soil drought on photosynthesis and chlorophyll fluorescence in bean plants". *Bulgarian Journal of Plant Physiology* 30.3–4, pp. 3–18.

Chapter 5: Appendix

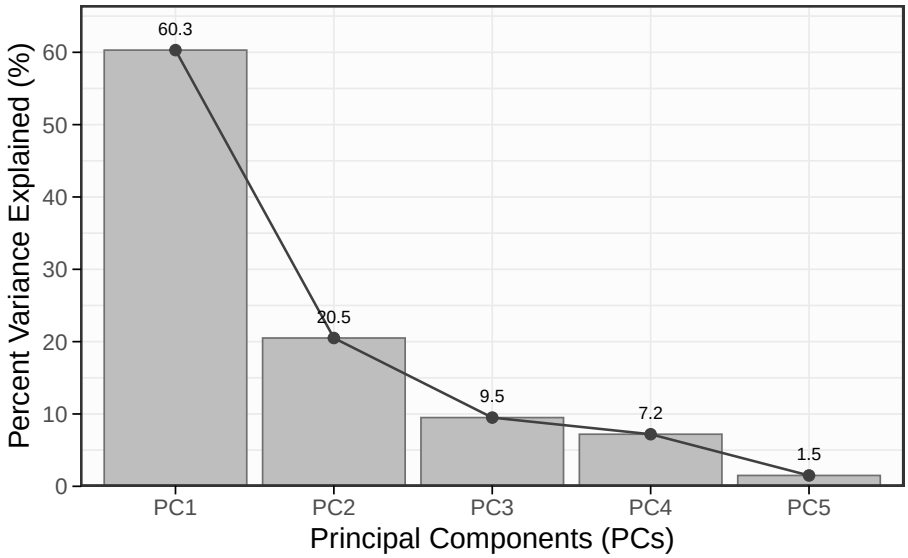

Supplementary Figure 5.1: Scree plot showing percent variance attributed to Principal Components of PCA analysis for OJIP FluorPen data of D1-10 plants. Biplot of PC1 and PC2 is shown in Figure 3.2(a).

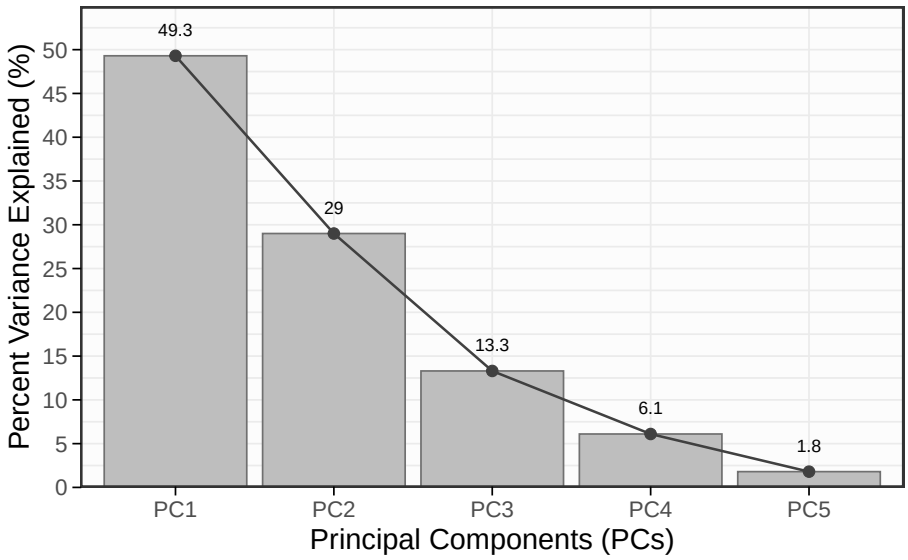

Supplementary Figure 5.2: Scree plot showing percent variance attributed to Principal Components of PCA analysis for OJIP FluorPen data of D1-40 plants. Biplot of PC1 and PC2 is shown in Figure 3.2(b).

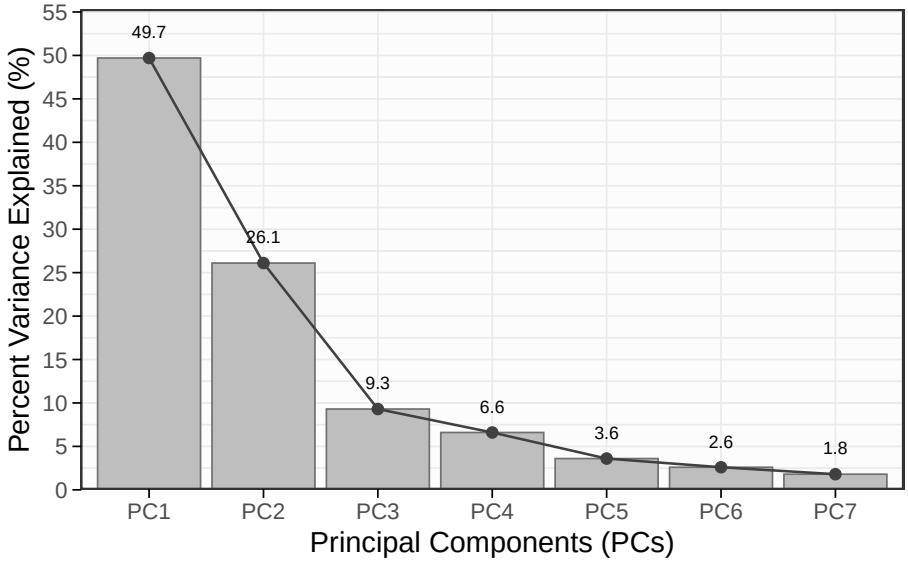

Supplementary Figure 5.3: Scree plot showing percent variance attributed to Principal Components of PCA analysis for OJIP FluorPen data of RW plants. Biplot of PC1 and PC2 is shown in Figure 3.2(c).

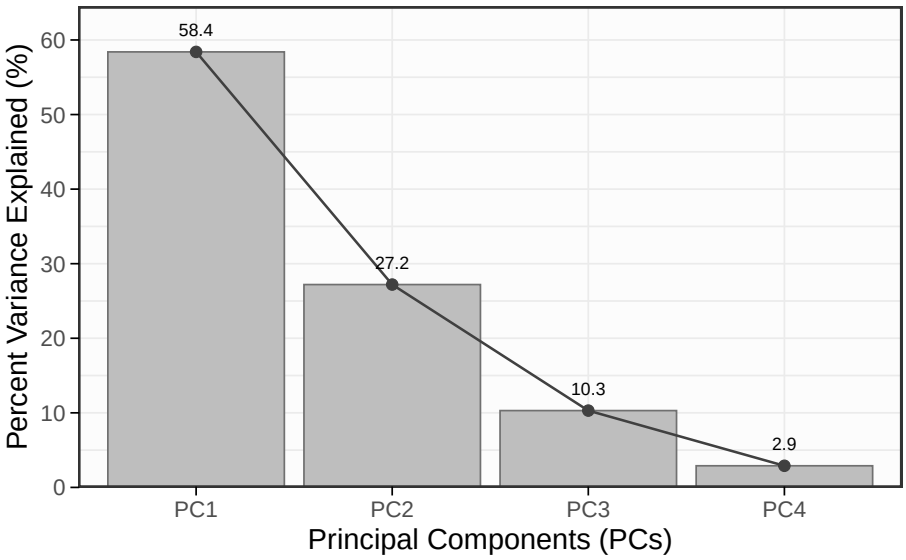

Supplementary Figure 5.4: Scree plot showing percent variance attributed to Principal Components of PCA analysis for OJIP FluorPen data of D2-10 plants. Biplot of PC1 and PC2 is shown in Figure 3.2(d).

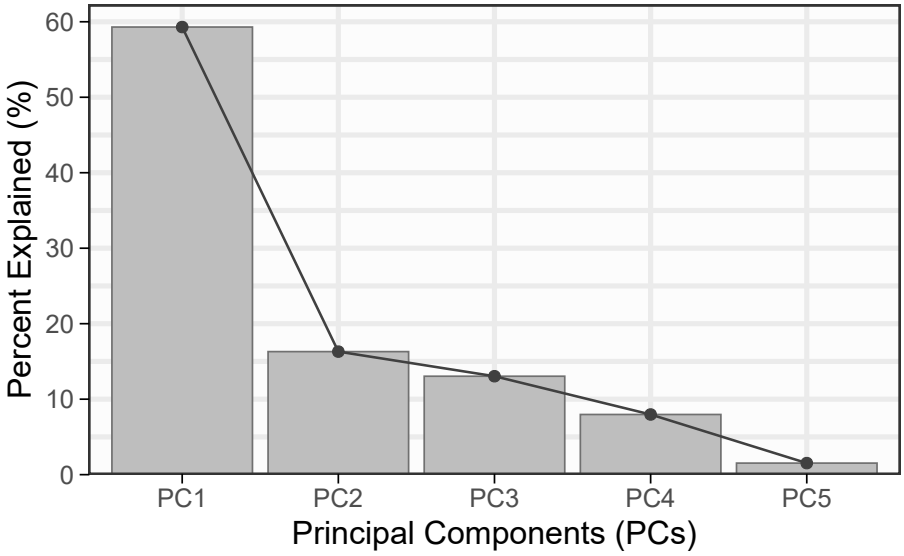

Supplementary Figure 5.5: Scree plot showing percent variance attributed to Principal Components of PCA analysis for OJIP FluorPen data of all stages of drought from Figure 3.10

Supplementary Table 5.1: First five Principal Component factor loadings at D2-10 for OJIP data of parental plants.

	PC1	PC2	PC3	PC4
$DI_O \cdot RC^{-1}$	-0.249	0.032	0.063	0.047
ϕ_{D_o}	-0.247	-0.049	0.045	-0.131
V_I	-0.245	-0.048	-0.076	-0.014
F_J	-0.245	0.036	-0.071	-0.138
M_O	-0.244	-0.036	-0.034	0.242
F_O	-0.241	0.082	0.058	-0.191
$ABS \cdot RC^{-1}$	-0.231	0.104	0.096	0.251
$TR_O \cdot RC^{-1}$	-0.215	0.138	0.110	0.350
F_I	-0.200	0.216	0.018	-0.176
V_J	-0.183	-0.228	-0.164	0.018
Fixed Area	-0.126	0.307	-0.015	-0.270
F_M	-0.121	0.313	0.049	-0.220
$\phi_{P_{av}}$	-0.083	-0.295	-0.088	-0.312
N	-0.040	-0.139	0.545	0.034
$ET_O \cdot RC^{-1}$	-0.009	0.315	0.256	0.271
F_V	-0.007	0.363	0.028	-0.170
HACH Area	-0.004	0.358	-0.060	-0.234
S_M	0.064	-0.205	0.466	-0.149
Area	0.071	-0.136	0.516	-0.208
ψ_o	0.183	0.228	0.164	-0.018
ϕ_{E_o}	0.203	0.202	0.123	-0.001
S_S	0.214	-0.135	-0.108	-0.373
π_{Abs}	0.236	0.123	-0.012	-0.129
$F_M \cdot F_O^{-1}$	0.245	0.057	-0.075	0.092
$F_V \cdot F_O^{-1}$	0.245	0.057	-0.075	0.092
$F_V \cdot F_M^{-1}$	0.247	0.049	-0.045	0.131
ϕ_{P_o}	0.247	0.049	-0.045	0.131